FINAL REPORT ON

RDU160336

Project Title:

Investigation of Thermal, Mechanical and Fracture Toughness Properties of Biodegradable Hybrid Nanocomposites

Project Leader
Ir. Dr. Mohd Bijarimi Bin Mat Piah

Co-Researcher
Prof Dr Mohammad Dalour Hossen Beg
Prof Rosli Bin Mohd Yunus

Faculty of Chemical and Natural Resources Engineering
Universiti Malaysia Pahang

October 2016

ABSTRACT

This work reports the preparation and characterization of poly(lactic) acid/acrylonitrile butadiene styrene/graphene nanoplatelets/Cloisite C20A montmorillonite (PLA/ABS/GnP/C20A) nanocomposites via melt blending. The clay is hybridized with graphene to increase its dispersion in the polymer matrix. The melt processing temperatures play a vital role in the properties of the resulting nanocomposites in dictating the extent of thermal stability and dispersion of the fillers. The hybrid nanocomposites were characterized for stress-strain, thermal, chemical, and morphological properties. The findings were that there was an increase in the mechanical properties in terms of tensile strength and Young's modulus with the PLA/ABS/GnP/C20A at the high-temperature profile having the highest values of 43.1 MPa and 2533 MPa. The elongation at break increases slightly, due to the brittle properties of GnP. It was found that the dispersion of the fillers increased with increasing temperature profiles, as revealed by the morphological analysis by scanning electron microscopy (SEM) and transmission electron microscopy (TEM). The void size was also observed to be smaller and more homogenous with increasing temperature. However, in terms of thermal degradation analysis, the addition of fillers increases its thermal stability as the decomposition onset temperature increases by 22.5°C.

CHAPTER 1

INTRODUCTION

1.1 Background

Nowadays, the search for polymers that are biodegradable and benign to the environment has been exploited by tailoring the existing commodity polymers. Poly(lactic acid) is a bioplastic made using renewable biomass known as poly(lactic acid) or called PLA. Renewable resources such as starch and sugar are one of the sources. PLA is an eco-friendly, biocompatible, and renewable polymer that can be processed using conventional processing equipment. Typically, the use of non-degradable plastics for consumer products and engineering goods has created a substantial dumping problem.

As such, polymers from renewable sources such as poly (lactic acid) (PLA) are on the threshold of gaining popularity. PLA has been extensively blended with other polymers to modify its inherent brittleness drawback, mainly rubber toughening, as demonstrated by previous research [1]. However, PLA is very brittle to be used commercially, and toughness modification is typically required. Various strategies have been employed to toughen brittle PLA, such as blending with plasticizers' and rubber/plastic blends [2-4]. In many cases, the strength and modulus of the toughened PLA are much lower than those neat PLA. PLA also a brittle thermoplastic with high strength and modulus, insufficient toughness, and low thermal stability.

Acrylonitrile butadiene styrene (ABS) is a tough material and suitable for toughening brittle PLA [5]. ABS is composed of acrylonitrile, butadiene, and styrene; it has strength and rigidity. The toughness property in ABS is contributed by the rubbery part of polybutadiene in the block copolymer [6]. ABS has been widely used for electrical and electronics goods, automotive parts, and household appliances. Recently, the use of ABS for 3D printing has increased tremendously, as many prototype developments require the aid 3D printer prior to commercialization. In the polymer blend of ABS/PLA, part of the ABS could be substituted with PLA in an effort to increase the content of the eco-friendly polymer. Li and Shimizu (2009) reported that the not compatibilized blends of PLLA and ABS blends exhibited poor mechanical properties with low elongation at break and impact strength [7]. However, they found that a reactive styrene/ acrylonitrile/glycidyl methacrylate copolymer (SAN-GMA) by incorporating ethyl triphenyl phosphonium bromide (ETPB) as the catalyst, SAN-GMA was an effective reactive compatibilizer for PLLA/ABS. The improvement in impact strength and elongation at break was attributed to the dispersion of rub ber particles in the blend. Choe et al. (2014) investigated the mechanical properties of acrylonitrile–butadiene–styrene copolymer/poly(l-lactic acid) (70/30) wt.% blends and their composites. They found that the SAN-g-GMA random copolymer was an effective compatibilizer for the ABS/PLA composites [8]. In another work by Dong et al. (2015) PLLA/ABS blend compatibilized by a reactive comb (RC) polymer, i.e. one poly- (methyl methacrylate) (PMMA) backbone, which was distributed randomly along the backbone. Their results showed that the improvement in toughness was most significant at the weight ratio of PLLA/ABS (50/50 %) [9]. In an effort to improve the toughness of PLLA, Wu et al. (2015) incorporated 6.0 wt.% ABS copolymer particles in a poly(L-lactide) (PLLA) matrix. They reported that the ABS copolymer increased the elongation yield at break and impact strength as compared to neat PLLA [10]. Vadori et al. (2016) explored polymer blends containing poly(lactic acid) (PLA) and acrylonitrile butadiene styrene (ABS) (50/50 %) blend. They found that acrylic copolymers and chain extender worked to synergistically increased the impact strength [5].

Polymer nanocomposites typically consist of nanofiller such as organomontmorillonite or graphene. Montmorillonite (MMT) is a cost-effective additive in polymers and currently the most researched filler for polymer composites. The use of MMT and graphene individually as nanofiller in the polymer matrix has been well established and available in the literature [11-24]. Nevertheless, there is a limitation for polymer nanocomposites based on MMT alone, such as brittleness and thermal conductivity. On the other hand, graphene is considered an ideal nano-reinforcement for multifunctional polymer nanocomposites owing to its extraordinary thermomechanical and electrical properties [25]. Even at a low load quantity of graphene, it can improve the overall mechanical properties of the polymer. Besides, graphene is expected to have significant characteristics such as high thermal conductivity, outstanding electronic transport properties, and more exceptional mechanical properties. Polymer

nanocomposites based on hybrid organomontmorillonite and graphene nanoplatelet (GnP) offers a new class of material by taking advantage of the performance of MMT and GnP as individual nanofiller. The synergistic effect of MMT and graphene functionalized epoxy in PLA blends was reported by Bouakaz et al. (2015). Their results showed that the enhancement of dispersion and exfoliation of two nanofillers (organomontmorillonite and graphene) in ternary PLA nanocomposites is ascribed to a right combination of repulsive and attractive interactions between the C15A-graphene and C30B-graphene systems [26]. It is very interesting to evaluate the hybridization effect of MMT/graphene for other types of blend systems such as PLA/ABS blends. In this work, part of the ABS was substituted with PLA in the ABS matrix in order to develop an ABS blend with 20% eco-friendly material. In addition, it was expected that the rigidity of the ABS blend could be enhanced by the presence of PLA, as a dispersed phase. The aim of this work was to prepare and characterize PLA/ABS with a hybrid of graphene and MMT as nanofillers in terms of mechanical, thermal, chemical, and morphological properties. The focus of the study is the effect of processing temperatures for three ranges of temperature profiles i.e. low, medium, and high temperatures.

1.2 Objectives

As there is huge potential of graphene as filler to strengthen the mechanical strength of Poly(lactic) Acid (PLA) nanocomposites, this research is carried out with two objectives:

- To prepare the PLA/ABS/GnP/C20A nanocomposite by using melt intercalation method.

- To investigate the effect of processing temperature profile on the mechanical, morphological and thermal properties of the PLA/ABS and PLA/ABS/GnP/C20A.

CHAPTER 2

LITERATURE REVIEW

2.1 Poly(lactic) Acid (PLA)

Poly(lactic) acid (PLA) is a renewable, sustainable, biodegradable, and eco-friendly thermoplastic polyester produced from renewable feedstock [25,27]. It has high potential for short-term applications as a disposable and degradable plastic with a wide end-use application due to its balanced properties of mechanical strength, thermal plasticity, and ability to be composted [27]. In fact, comparing with conventional polymers such as polypropylene (PP), polystyrene (PS) and polyethylene (PE), in terms of mechanical strength, PLA possess much superior tensile Young's modulus, tensile strength and flexural strength [28].

However, for PLA to be use in large scale commercial application, first and foremost, its inherent brittleness, poor thermal resistance and limited gas barrier properties has to be addressed. The brittleness of PLA can be seen in its elongation at break and impact strength which is inferior to the aforementioned conventional polymers [28]. For applications that require injection moulding, blow moulding, thermoforming or extrusion, adequate thermal stability are required to maintain molecular weight properties and prevent degradation [29].

In addition, although, in recent years, low-cost industrial processes had been developed, PLA remains expensive in comparison to the common synthetic petrochemical polymers. According to Nampothiri et. al. (2010) to compete with the common synthetic petrochemical polymers, the manufacturing cost should be targeted below 0.8 US$/kg. This is because the market price needs to be reduced by half of the current price of 2.2 US$/kg. To achieve this, he commented that the issues that need to be addressed are the high-performance lactic-acid producing microorganisms' development and the cost reduction of the raw materials and fermentation process.

In a nutshell, the commercial success of PLA is highly dependent on two crucial factors; reducing cost and improving the polymer property especially in food industry. Nuona et. al. (2014) believes that this could be by incorporating specific fillers into the PLA matrices [27].

2.2 Acrylonitrile Butadiene Styrene (ABS)

While normal acrylonitrile butadiene styrene ABS, can be blended with PLA, high rubber ABS (50-85% rubber) content, also known as ABS grafted rubber concentrates, and have found to successfully strengthen PLA (NatureWorks, 2007). The two polymers

possess similar melt processing temperatures and thus are easily capable to be processed via standard melt mixing equipment. Due to their immiscibility, the blend produced is opaque and the physical and thermal properties it possesses is as expected for two phase blends. From table 2-1, it can be seen that the impact strength of PLA/ABS composite is better than in neat PLA.

Table 0-1 Injection Moulded Properties of Some PLA Blends with Commercial Polymers (NatureWorks 2007)

	% Polymer in PLA Blend	Tensile Yield[e] (psi)	% Elong.[e]	Tensile Modulus[e] (psi)	DTUL[f] °C @ 66 psi	Izod Impact[g] (ft-lbs/inch)	Clarity
Polycarbonate[a]	20	9,130	3.0	411,000	59	0.35	No
PMMA[b]	20	9,730	4.0	453,400	58	0.33	Yes
	50	10,575	4.0	453,900	63	0.32	Yes
	80	10,625	5.1	446,500	73	0.29	Yes
ABS[c]	20	7,950	2.9	414,000	58	0.48	No
	50	7,130	2.5	377,700	61	0.29	No
	80	6,660	4.9	343,000	89	0.59	No
PLA[d]	100	9,150	3.5	429,500	59	0.35	Yes

Caliber™ 200-22 b. Magnum™ 555 c. Paraloid ™ CA 86 d. NatureWorks® 2002D e. ASTM D638 @0.2 inch/min. f. ASTM D648-06 g. ASTM D256-92

In terms of elongation at break, although at lower ABS loading, the value is low, increase in ABS loading improves the elongation at break due to the ABS ductile properties. In addition, Sun et. al. (2011) also found that the incorporation of ABS-grafted glycidyl methacrylate (ABS-g-GMA) as the toughening agent could enhance the impact strength and elongation at break of PLA [30].

2.3 Nanofillers

Nanofiller is filler with at least one dimension lies in the range of 1–50 nm which is dispersed into the polymer matrix to form nanocomposite. Fillers was initially used to reduce cost of the polymeric product but is now became an integral part in many applications, especially polymer mechanical properties reinforcement [31].

2.3.1 GRAPHENE

Graphene is a 2-dimensional (2D) material of one atomic-layer thick honeycomb sheet of carbon atoms that makes up the fundamental structural unit of some carbon allotropes, such as graphite, carbon nanotubes and fullerenes. As the basic building, stacked layers of graphene of more than 20 thicknesses made up graphite. On the other hand, rolling them along a given direction made up nanotube. As for fullerenes, wrapping-up the graphene produces a zero-dimensional fullerene [32]. Figure 2-1 shows the different carbon allotropes.

Although the perception of graphene was noticed by Brodie in 1859 from the highly lamellar structure of thermally reduced graphite oxide, the theory of graphene had only been first explored in 1947 by P.R. Wallace [33]. However, only by 2004 was graphene truly discovered by the physicists Sir Andre Geim and Sir Konstantine Novoselov in a ground-breaking experiment that had won them the Nobel Prize in 2010. This discovery includes the unique behaviour attributed to a number of exceptional phenomena in graphene leading dramatic growth of interest in this field [34].

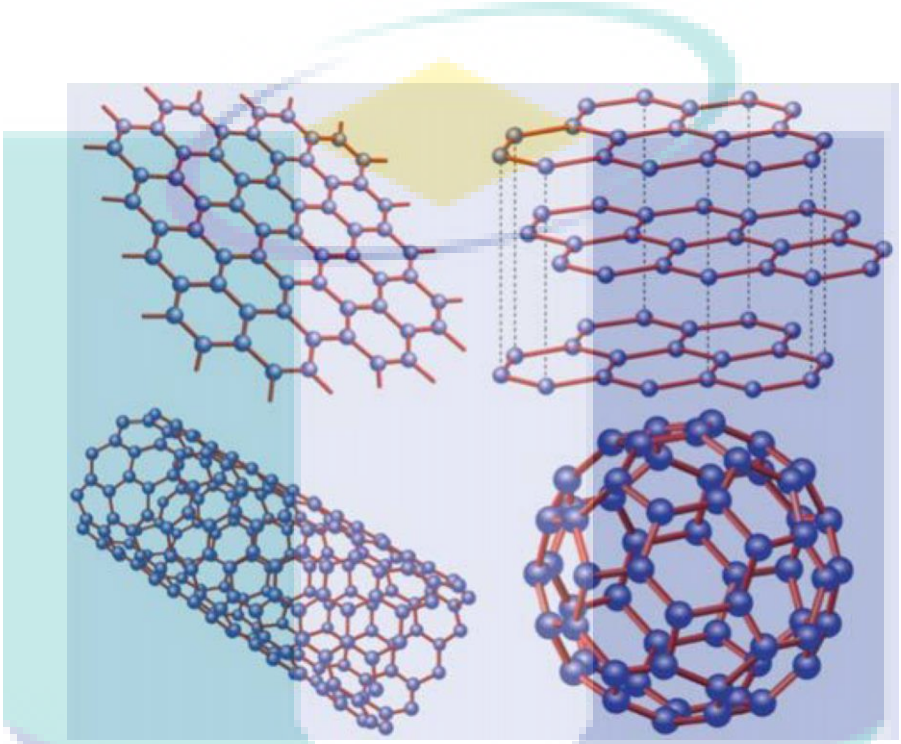

Figure 0-1 Top left: Graphene, a honeycomb lattice of carbon atoms. Top right: Graphite, a stack of graphene layers. Bottom left: Carbon nanotubes, rolled-up cylinders of graphene. Bottom right: Fullerenes (C60), wrapped graphene achieved through the introduction of pentagons on the hexagonal lattice (Reproduced with permission from [32].

The graphene outstanding properties in terms of thermomechanical and electrical makes it the finest nano-reinforcement for multifunctional polymer nanocomposites. Graphene possess the top elastic modulus of 1 TPa. The thermal conductivity is also very at 5.1×10^{3} $Wm^{-1}K^{-1}$. In addition, at with intrinsic electrical conductivity 6×10^{5} Sm^{-1}, graphene is the greatest known material possessing such value. It is also worth to note the individual graphene sheet van der waal thickness is 0.34 nm, making it the thinnest 2D nanofiller recognized to date. Graphene also has tremendously high aspect ratio of flakes (ratio of lateral dimensions to thickness of 10^{4} and upper) and great intrinsic flexibility. Recent research also found that graphene that does not possess oxides or other functional group, particularly pristine graphene, has a very good biocompatibility [35]. Conroy et. al. (2014) stresses that this implies toxicity potential only appears after chemical treatment since the toxicity reported by previous studies uses graphene that has been chemically modified like graphene oxide (GO). GO possess many oxygen atoms in the form of carboxyl groups, epoxy groups and hydroxyl groups.

However, according to Hu et. al. (2014), since pristine graphene are hard to synthesis and its mass production requires high time and energy consumption, research are more focused on other variant of graphene that partially preserve the exceptional properties of graphene. The focus on the derivatives of graphene is also due to the fact that some of them possess quality that overcomes some of pristine graphene deficiency. In addition, hydrophobic nature of pristine graphene makes it tends to agglomerate in polymer matrix [33]. Although the hydrophobicity and π-π interaction could be utilised for effective drug loading, graphene poorly dispersed in water.

2.3.2 NANOCLAY

Nanoclay can be in the form natural or synthetic clay as well as in the form of phosphates of transition metals [36]. As filler, nanoclays attributes to overall improvement in physical performances of nanocomposites. It possesses high mechanical strength with a single sheet of montmorillonite having Young's modulus in the range of 178 to 265 GPa [31].

Clay of 2:1 layered or phyllosilicates structural family (as shown in Table 2-2) is the most used clay in polymer/clay [36,37]. It has a sheet structure in which layers of octahendral sheet of alumina or magnesia packed between two tetrahedral sheets of silica made up their crystal structure. The structure of 2:1 phyllosilicates are illustrated as in Figure 2-2. Subjected to the particular layered silicate, the lateral dimensions may differ from 30 nm to several micrometres and even larger with layer thickness of ~ 1 nm. The layers leads to arrange themselves to form stacks with a regular Van der Waals gap between the layers called the interlayer or gallery. To retain charge neutrality, isomorphic exchange within the layers of pristine clay generates negative charges that are counterbalanced by alkali and alkaline earth cations (Na^+ , Li^+ , Ca^+) situated inside the galleries.

Table 0-2 Classification of clay mineral (phyllosilicate) [38].

Type	Group	Groupoid	Species	Tetrahedron	Octahedron	Interlayer cation
2:1$Si_4O(OH)_2$	Pyrophylite talc (x≈0)	di.	Pyrophylite	Si_4	Al_2	-
		tri.	Talc	Si_4	Mg_3	-
	Smectite (0.25<x<0.6)	di.	Montmorillonite	Si_4	$(Al_2,Mg)_2$	Na, Ca, H_2O
		di.	Hectorite	Si_4	$(Mg_2,Li)_2$	Na, Ca, H_2O
		di.	Beidite	$(Si,Al)_4$	Al_2	Na, Ca, H_2O
		tri.	Saponite	$(Si,Al)_4$	Mg_3	Na, Ca, H_2O
	Vermiculite (o.25<x<0.9)	di.	Vermiculite	$(Si,Al)_4$	$(Al_2,Mg)_2$	K, Al, H_2O
		tri.	Vermiculite	$(Si,Al)_4$	$(Mg_2,Al)_3$	K, Mg, H_2O
	Mica (x≈1)	di.	Muscovite	$Si_3.Al$	Al_2	K
			Paragonite	$Si_3.Al$	Al_2	Na
	Brittle mica (x≈2)	tri.	Phlogopite	$Si_3.Al$	$(Mg,Fe^{2+})_3$	K
			Biotite	$Si_3.Al$	$(Fe^{2+},Mg)_3$	K
2:1:1$Si_4O_{10}(OH)_8$	Chlorite (large variation of x)	di.	Donbassite	$(Si,Al)_4$	Al_2	$Al_2(OH)_6$
		di.-tri.	Sudoite	$(Si,Al)_4$	$(Al,Mg)_2$	$(Mg,Al)_3(OH)_6$
		tri.	Clinochlorite	$(Si,Al)_4$	$(Mg,Al)_3$	$(Mg,Al)_3(OH)_6$
			Chamosite	$(Si,Al)_4$	$(Fe,Al)_3$	$(Fe,Al)_3(OH)_6$
	Kaoline mineral serpentinite (x≈0)	di.	Kaolinite	Si_2	Al_2	-
			Halloysite	Si_2	Al_2	H_2O
		tri.	Chrysotile	Si_2	Mg_3	-
Needle	Sepiolite palygorskite (x≈0)	tri.	Sepiolite	Si_{12}	Mg_8	$(HO_2)_4.H_2O$
			Palygorskite	Si_8	Mg_8	$(HO_2)_4.H_2O$
Amorphous-low crystalline			Imogolite	SiO_3OH	$Al(OH)_3$	-
			Allophane	(1-2)SiO_2.(5-6)H_2O		
			Hisingerite	SiO_2-Fe_2O_3-H_2O		

X degree of isomorphous substitution; di.: dioctahedral; tri.: triotahedral

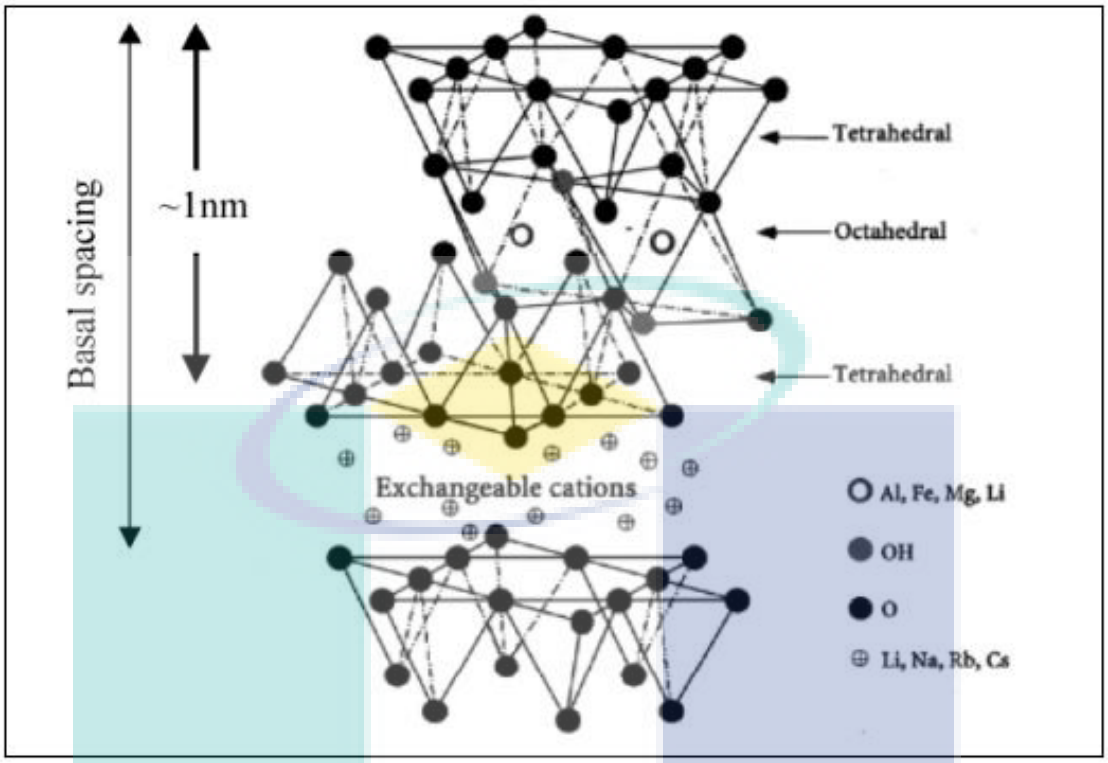

Figure 0-2 2:1 phyllosilicate structure [39].

The cation exchange capacity and layer morphology (crystalline structure) of the clay are used to characterize the type of clay. According Kamal (2010) and Marquis et. al. (2011) the cation exchange depends on the quantity and position of the ions within the elementary mesh and thus to characterize it, an average value of the charge over the whole crystal has to be considered as the charge is not locally constant, but differ from layer to layer. Montmorillonite, saponite and hectorite are the most used layered silicate. The characteristic and chemical formula can be seen in Table 2-3. For polymer nanocomposite design, the smectite clays are the materials of choice due to their exceptional rich intercalation chemistry. This allows chemical modification of the clay, ensuring compatibility with organic polymers for dispersal on a nanometre length scale. They are cheap and easy to obtain in mineralogical pure form as it is abundance in nature. The layered silicate consist of two types of structure; tetrahedral-substituted and octahendral-substituted. The polymer matrices are more readily to interact with tetrahedrally substituted material than with octahendrally-substituted material due to the location of the negative charge being on the silica layers' surface.

Table 0-3 Chemical formula and characteristic parameter of commonly used 2:1 phyllosilicate [40]

2:1 phyllosilicate	**Chemical formula**	**CEC (mequiv/100g)**	**Particle length (nm)**
Montmorillonite	$M_x(Al_{4-x}Mg_x)Si_8O_20(OH)_4$	110	100 – 150
Hectorite	$M_x(Mg_{6-x}Li_x)Si_8O_20(OH)_4$	120	200 – 300
Saponite	$M_xMg_6(Si_{8-x}Al_x)Si_8O_20(OH)_4$	86.6	50 – 60
M, monovalent cation; x, degree of isomorphous substitution (between 0.5 and 1.3)			

According to Kamal (2010), two vital factors in choosing clay for polymer layered silicate nanocomposites are their ability to disperse into individual layers and to adjust their surface chemistry via ion exchange reactions with organic and inorganic cations to form organophilic clay which are interrelated to each other. This is due to the fact that the interlayer cations affect the degree of dispersion of layered silicate in a particular polymer matrix. The nature of these clays are originally hydrophilic making them only able to interact with hydrophilic polymers, such as poly(vinyl alcohol) (PVA) and poly(ethylene oxide) (PEO). To improve their compatibility with many matrices of engineering polymers by, modification has to be made by increasing the organophilicity of the clay . Cation exchange, silane grafting and adsorption of polar polymers are some of the way the clay can be modified. Among these three, cation exchange is the method mostly employed. However, this method is highly dependent on the crystal size, pH and type of exchangeable ions.

Depending on the cation exchange capacity of the clay, the ion exchange reaction with cationic surfactants may comprise of primary, secondary, tertiary, and quaternary alkyl ammonium or alkylphosphonium cations. Alkylammonium or alkylphosphonium cations is used in the organosilicates to reduce the surface energy of the inorganic host and increase the wetting characteristics and intercalation with the polymer matrix, resulting in a larger interlayer spacing [41]. In addition, the functional groups that may be provided by the alkylammonium or alkylphosphonium cations could allow chemical reaction with the polymer matrix. In some cases, monomer polymerisation may even be initiated to enhance the interface adhesion strength between the polymer matrix and the clay nanolayers. The hierarchical morphology contained in most layered silicates, be it organically modified or not, can be defined by three general levels of structure; crystallite (tactoid), primary particle and agglomerates as shown in Figure 2.3. Up to 100 individual layers can be found stacked together in the crystallite which can also be commonly referred to as tactoids. Dense face to face stacking or low angle intergrowth of individual tactoids is entailed in the primary particles. Finally, the powder that we generally refer to as particles are formed from the weak agglomeration of these particles. To achieve homogenous nanoparticles and dispersion in the matrices of the polymer, disruption of the tactoids as well as primary particles and the agglomerates' dispersion are vital.

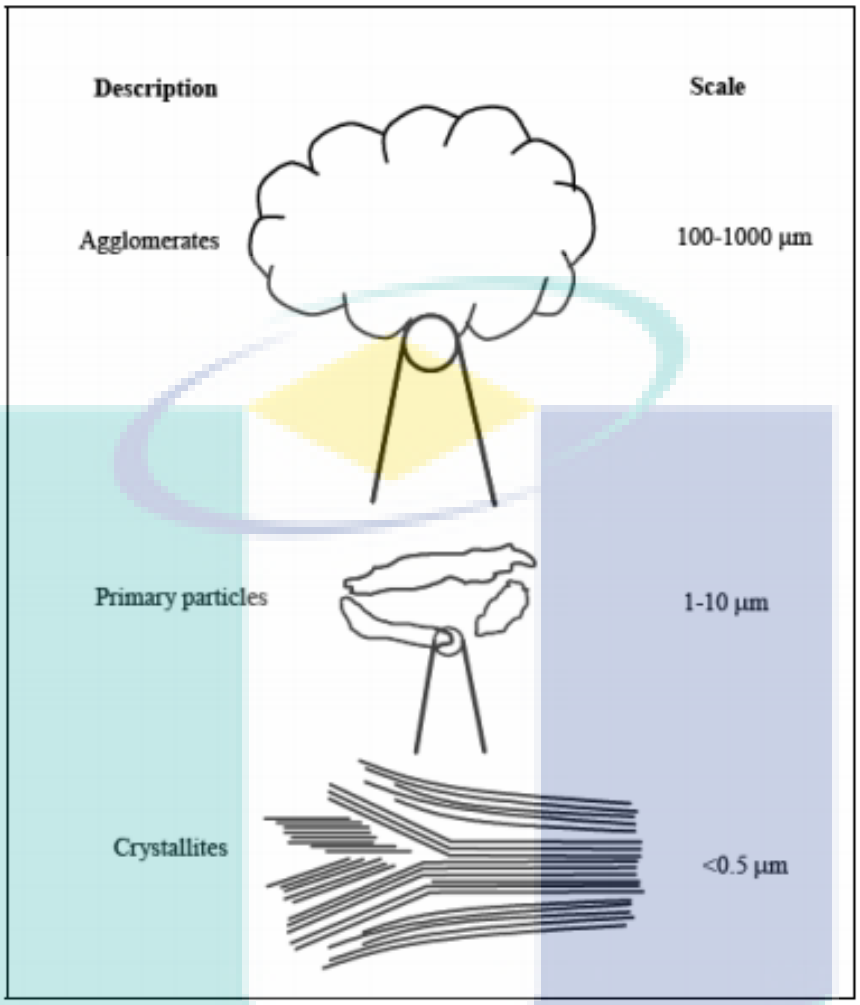

Figure 0-3 Montmorillonite clay particles hierarchy [42]

2.3.3 HYBRID GRAPHENE/NANOCLAY

The hybridization of graphene with 2D materials, for example montmorillonites, had been found to enhance carbon nanotubes' dispersion, which is carboceous material, in recent studies. According to the available literature, the synergistic effect makes these hybrid-filled polymer nanocomposites to display excellent properties in comparison to polymer with individual fillers [43].

Fukushima et. al. (2010) studied the effect of fusing two nanofillers by incorporating expanded graphite and Cloisite 30B (C30B) in PLA. The results show enhancement of mechanical properties, thermal stability, and fire-retardant properties. They claimed that these improvements were attributed to the decent (co) dispersion and to the nanoparticles reinforcement effect. Apart from that, the remarkable improvement was also noted by many researchers in terms of modulus, strength, barrier property, resistance to flame, and thermal stability of both montmorillonite and organically modified montmorillonite (OMt) reinforced polymer when compared to conventional composites [44-46].

2.4 Preparation of Polymer

The two crucial factors in preparing PLA nanocomposites with the desired properties enhancements are the compatibility and the effective dispersion of the fillers. The resulting nanocomposite will exhibit inferior properties to the predicted ones in case of failure in achieving either one of these things. Apart from that, it is also vital to pay attention to the significance of materials preparation as failure may result in an incorrect conclusion that the poor silicate dispersion and/ or materials performance are due to the compatibilization strategy. The methods that are mostly used to prepare polymer composites are solution intercalation, melt intercalation and in situ polymerization. However, in this paper, only melt intercalation method will be discussed.

As of late, the melt intercalation technique has been the main conversion technique for PLA. Najafi et. al. (2012) stated that this is due to the fact that it requires no solvent as well as being compatible with the current industrial compounding and processing technique. This is because melt intercalation method is a solvent free method in which the fillers are distributed in the polymer matrix via mechanical shear force using a screw extruder or a blending mixer [47]. The mixing is usually in molten state and are performed at elevated temperatures [48]. To form nanocomposites, intercalation or exfoliation need to be achieved on the polymer chain.

In terms of commodity polymers, this method is widespread and has broad applications (Kamal, 2010). There are many advantages of using this method. The absent of solvent makes it environmentally benign as well as economical in term of cost [49]. In addition, unlike in solution and in situ intercalation that requires compatible polymer-filler solvent system, through the hybrid process, melt intercalation technique is highly open to a variety of challenging polymer.

The melt intercalation technique has been successful with polymer/clay nanocomposites due to the clay's and the polymer's affinity. Some of the success polymer nanocomposites intercalation includes PP, PS, low density polyethylene (LDPE), high density polyethylene (HDPE), polymethyl methacrylate (PMMA) and, of course, PLA. The shear force in melt intercalation also leads to better dispersion and properties enhancement.

On the other hand, Bhattacharya (2016) suggested that the difficulty of melt intercalating polymer/graphene nanocomposites are due to fact that most chemically modified graphene has low thermal stability in addition to graphene itself having low bulk density. This is supported by Fu et. al. (2014) who finds that the stable the single sheet dispersion graphene in polymer matrix is extremely difficult to attain due to high strength inter-sheet Van der Waals force and large area-to-volume ratio of graphene. The mechanical properties of the resulting nanocomposite will be poor if the dispersion of the graphene in the polymer matrix is poor. This is because poor dispersion and excessive aggregation results in a reduced interfacial area and weakened interfaces.

Figure 2-4 shows the different scenario that could occur during the fabrication of polymer nanocomposite with laminated reinforcing materials. The improvement of the interfacial strength and spectacular enhancement of the interfacial area, resulting in stronger nanocomposite materials can be achieved through efficient exfoliation of stacked laminates followed by intercalation. Stronger interfacial interactions and a localized improvement in the properties can be obtained from efficient intercalation

making it important to achieve homogenous dispersion and exfoliation of graphitic components inside the polymer matrix for better performance [32].

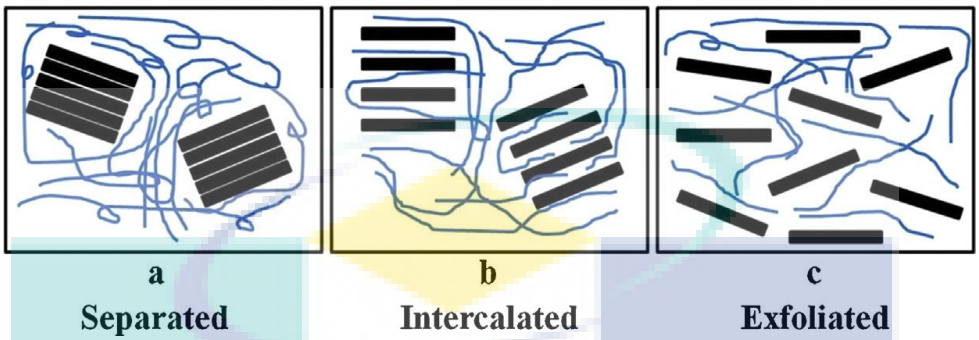

Figure 0-4 Dispersing scenarios of laminated nanofillers in polymer matrix representative [32].

Note also that for melt intercalation to succeed, the process must be performed at temperature higher than the glass transition temperature of amorphous polymer components (ABS in this case) and temperature higher than the melting point of PLA (the semi-crystalline polymer component). This is to be able to manage the viscosity and to attain optimum dispersion. For PLA blends, the processing temperature should be in the range of 180^{o}C and to 270^{o}C. The lower limit is to ensure the polymer is in molten and the upper limit is to prevent thermal degradation. To enhance mixing, modification of the process condition can be done on either the compounding temperature or the components' molecular weight. In order to obtain good mixing, the condition of the equipment and screw design also needs to be considered. Optimization should be done on the rotation per minute (RPM) of the screw, feed rate and other process conditions. The components also needs to be thoroughly dried prior to processing as PLA is very sensitive to polymers that have nucleophilic additives or contain high levels of water which can cause molecular weight loss of the PLA resulting in blends with poor physical properties (NatureWorks, 2007).

2.5 Physical and Mechanical Properties of Nanocomposites

2.5.1 PLA/NANOCLAY

In terms of elongation at break, Jollands & Gupta (2010) found that at clay loading of 4wt%, the elongation at break of PLA nanocomposite increase from 2.3% (in pristine PLA) to 3.2%. This is supported by Gamez-Perez et. al. (2011), as they found that addition of OMt increases the elongation at break from 4.0% to 5.7% and 11% for clay loading of 0.5wt% and 2.5wt% [50]. Another research by Wang et. al. (2012) also found similar results with increment from 5.4% to 7.9% at 1wt% clay loading [51]. Lai et. al. (2014) stated that the highest improvement in literature was achieved by Li et. al. (2009) with result of 26.5 times enhancement in comparison with pristine PLA. However, in their own research, Lai et. al. (2014) had actually achieved 37-fold increment in the elongation at break with addition of 1 phr of C30B.

In terms of thermal properties, Paul et. al. (2003) found that the maximum thermal stability increment can be achieve at 5wt% of clay as further increment of the clay loading decreases the thermal stability due to the relative extent of exfoliation/delamination in function of amount of organo-clay. Increasing filler content increases relative exfoliation of individual particles, increasing thermal stability. However, at 5wt%, complete exfoliation gets hindered by geometrical constraint within the limited space in the polymer matrix resulting in decrease of thermal stability [52].

Biodegradation increase with addition of clay, with the research by Ray et. al. (2002) found that the PLA/oligomeric polycaprolactone (O-PCL) blended with clay mineralised completely within 60 days in industrial compost. They suggested that this is due to the presence of terminal hydroxylated edge group of the silicate layers.

2.5.2 PLA/GRAPHENE

In general, graphene can enhance mechanical and thermal properties of PLA. It had been reported that the mechanical and thermal stability of polymer substantially increases with only 0.2 mass% incorporation of lyophilized graphene nanosheets (GNs) into PLA [53]. In another research by Pinto et. al. (2013), in comparison to pristine graphene, higher yield strength, Young's modulus and impermeability of PLA be obtained by incorporating even small amounts (0.2 to 1 mass%) of GO and graphene nanosheets [54]. In PLA or plasticized PLA, the thermal stability and tensile strength is substantially enhanced by the adding reduced GO and graphene nanosheets without decreasing its elasticity was recently concluded by many researchers. However, they stated that graphene nanosheets have the tendency to agglomerate, resulting in poor dispersion in the polymer matrices in melt intercalation [55]. This may restrict the development of graphene as nanofiller in polymer nanocomposite

Kim & Jeong (2010) investigated the morphology, structure, thermal stability, mechanical, and electrical properties of PLA/exfoliated graphite nanocomposites in comparison to PLA/micron-sized natural graphite (NG) composites. SEM images and XRD patterns performed following melt-compounding with PLA matrix, verified that exfoliated graphite, having thickness of 15 nm, were dispersed homogeneously in the PLA matrix. This finding disagrees with the agglomeration seen in the case of NG. With graphene content up to 3wt%, the thermal degradation and Young's moduli of PLA/exfoliated graphite improved considerably. On the other hand, no significant changes observed with the PLA/NG regardless of the micron-sized graphite content [56].

In terms of tensile strength, Mat Desa et. al. (2014) found that the tensile strength of PLA nanocomposite increase slightly with addition of 3 phr of CNT and later increase significantly at 5 phr. However, the value decreases at 7 phr due to inevitable aggregation. The Young modulus was also found to inhibit increasing strength with increasing loading with 180% increment at 7 phr in comparison to pristine PLA. However, it was found that the toughness drops at increasing filler loading with 24.09% decrement in impact strength at 1 phr in comparison with pristine PLA [57].

In terms of biodegradability, Paul et. al. (2005) found that the addition of nanoclays into PLA has also shown higher biodegradability in compost. They claimed that this is due to increase in water permeability attributed by the high relative hydrophilicity of the clay, leading to easier permeability of water to activate the hydrolytic degradation process.

2.5.3 PLA/GRAPHENE/NANOCLAY

In terms of rheology, a research by Bouakaz et. al. (2015) studied the synergy between graphene/clay nanofiller in PLA using two combination of graphene functionalized epoxy with Cloisite 15A (C15A) and Cloisite 30B (C30B) and found that the filler-polymer and filler-filler interactions result in improved complex viscosity. The better the dispersion of the nanofillers, the larger the interfacial area, thus, yielding a higher fraction of polymer chains that could interact with the filler particles. This in turn increases the dynamic volume. The storage modulus of the system also significantly enhanced signifying a three-dimensional (3D) network formation and decent state of dispersion of the filler mixtures. The reinforcing factors were also significantly improved due to higher dispersion of nanofillers, with the non-polar OMt (C15A) showing better performance than the polar filler. Another research, Boakaz et. al. (2017) studied the effect of combination of graphene functionalized epoxy with Cloisite 15A and 30B in PLA/PCL blend and found a similar result with C15A being better at dispersion than C30B. They stated that this finding were similar with other non-polar OMt's like C20A in the experiment by Li et. al. (2011).

CHAPTER 3

METHODOLOGY

3.1 Materials

Materials required to run these experiments are PLA, ABS, graphene platelets (GnP) and Cloisite 20A (C20A). PLA 3251D acquired form NatureWorks have a density of 1.24g/cm3. The melting temperature (Tm) is between 155oC to 170oC with glass transition temperature (Tg) of 55oC to 60oC. ABS TOYOLAC 700 314 acquired from TORAY Plastic Malaysia have a glass transition temperature of 103oC with no true melting temperature due to amorphous nature. The C20A was received from Southern Clay Products, Inc. For the melt intercalation blending of the nanocomposites, a twin-screw extruder was used. A film block mould was also attached at the end zone for moulding.

3.2 Blend Composition

For the blank, the composition of the blend will be fixed at 90g:10g of PLA/ABS while for the tested specimens. Then, the filler, GnP:C20A is added at 2w% of the composition at ratio of 1:1.

Polymer blend formulation will be compounded by adding PLA/ABS/GnP/C20A blends that has been physically mixed prior to feeding into the twin-screw extruder. The temperature of each zone inside the extruder is set as follows:

Table 0-1 Temperature Profile for PLA:ABS composites

Twin Screw Extruder Zone	**2**	**3**	**4**	**5**	**6**	**Die**
Low Temperature Profile (LT) (°C)	190	180	180	175	165	160
Medium Temperature Profile (MT) (°C)	200	190	190	180	170	160
High Temperature Profile (HT) (°C)	210	200	200	185	170	160

Table 0-2 Temperature Profile for PLA:ABS:GnP:C20 nanocomposites

Twin Screw Extruder Zone	**2**	**3**	**4**	**5**	**6**	**Die**
Low Temperature Profile (LT) (°C)	190	180	180	175	172	168
Medium Temperature Profile (MT) (°C)	200	190	190	180	175	168
High Temperature Profile (HT) (°C)	210	200	200	190	180	168

The screw rotation speed was maintained at 50 rpm. After blending, produced nanocomposite exiting the extruder will directly moulded into a homogenous film measuring about 20 mm wide with average thickness between 0.3 mm to 0.5 mm via the moulder attached at the end of the extruder.

3.3 Characterization

3.3.1 Fourier Transforms Infrared Spectroscopy (FTIR)

The chemical changes after blending were monitored by FTIR spectroscopy. The IR spectra were recorded using a PerkinElmer Spectrum 400 FT-IR spectrometer with 4 cm^{-1} resolution and 10 scans. All spectra were recorded in the transmittance mode in the 4000–600 cm^{-1} region.

3.3.2 Mechanical Testing

All compositions of the blend were tested and compared in terms of their mechanical properties. The tensile test was carried out according to ASTM D638 using a Testometric M350-10CT tensile machine (Testometric Company, Ltd. UK.) under ambient conditions with

crosshead speeds of 50 mm min^{-1}. The stress-strain properties values are taken from an average of five specimens.

3.3.3 Fracture Morphology

Scanning electron microscope (SEM) observation was performed on tensile fracture surface using a LEO 1450 VP SEM. Prior to the microscopy observation, the fractured surfaces were sputter coated with a thin layer of gold.

In the case of transmission electron microscope (TEM), the tensile fracture specimen was trimmed into a trapezoidal shape and sectioned using Ultramicrotome (Leica EM UC7) at -100^{0}C. The specimen was deposited onto the copper grid and observed by TEM (Tecnai G2-20) at an acceleration voltage of 40 to 200kV.

3.3.4 Thermal Analysis

3.3.4.1 Differential Scanning Calorimetry (DSC)

Differential scanning calorimetric (DSC) measurements were performed under a nitrogen atmosphere on samples of 5–8 mg using a Mettler Toledo DSC 822 (Mettler Toledo (M) Sdn. Bhd.) apparatus. The sample was heated at 25°C to 200 °C at a scan rate 10°C /min. The glass transition (T_g), crystallization temperature (T_c) and melting temperatures (T_m) were determined. Polymer crystallinity was determined with DSC by quantifying the heat of fusion of the polymer. The degree of crystallinity (X_c) of blend was calculated from the following equation:

$$X_c = \frac{\Delta H_m}{\Delta H_m^0} \times 100\%$$

where ΔH_m is the melting enthalpy of PLA and LLDPE homopolymer appear in a heating cycle. $\Delta H_m^o = 93 J/g$ and $\Delta H_m^o = 140.6\, J/g$ is the melting enthalpy of 100% crystalline PLA and LLDPE respectively [i,ii].

The partial crystallinity of blend components (PLA and LLDPE) in the blend is also calculated theoretically by using the following relation [iii].

Theoretical Crystallinity (C_{rth}) (%) =Percent crystallinity of pure component $\times W$(weight fraction of component)

3.3.4.2 Thermogravimetric Analysis (TGA)

Thermogravimetric analysis (TGA) is a technique that measures the mass and the change of mass of the sample during heating as a function of time and temperature. The evaluation of thermal stability of PLA and blends was carried out with a Mettler Toledo TGA/SDTA 851 apparatus (from Mettler Toledo (M) Sdn. Bhd). Samples were heated from 35 °C to 600 °C at a scanning rate of 10°C min^{-1} under a nitrogen atmosphere.

CHAPTER 4

RESULTS AND DISCUSSION

4.1 Mechanical Properties

Table 4.1 summarises the mechanical properties of the PLA, ABS, PLA/ABS and PLA/ABS/GnP/C20A nanocomposites. The temperature was denoted by the abbreviation LT, MT and HT for low temperature, medium temperature and high temperature respectively. The properties of PLA and ABS were obtained from literature while the nanocomposites were obtained from mechanical testing. Note that there is no data available for PLA/ABS LT due to inferior mechanical properties and thus specimen could not be prepared. The reduction in mechanical properties of the nanocomposites in comparison with the neat polymers is expected as the polymer is of physical blends. In terms of mechanical properties across the different nanocomposites, it was expected that the tensile strength, elongation at break and Young's modulus should increase with increase of temperature. From Figure 4.1-4.2, this is evident with PLA/ABS/GnP/C20A HT showing the highest value in the stress-strain curves.

From the Figure 4.1, the tensile strength, as represented by the stress at peak, shows that the PLA/ABS/GnP/C20A has better performance in comparison with the PLA/ABS nanocomposites with the exception of PLA/ABS/GnP/C20A LT. There is increase of 20% and 16% observed when comparing the PLA/ABS and PLA/ABS/GnP/C20A at MT and HT profile respectively. The addition of nanofillers had been demonstrated in other literature such as findings by Fukushima et. al. and Boakaz et. al. [58,29]. In addition, the tensile strength was also observed to be increased with increasing temperature. This is because increase in temperature increases the kinetic energy required to overcome the immense Van der Waals forces between the GnP structure allowing a better dispersion in the polymer matrix. The drop in tensile strength in PLA/ABS/GnP/C20A LT lower than the PLA/ABS nanocomposites could be due the agglomeration of the nanofillers as discussed in MMT/GNP dispersion and morphology section.

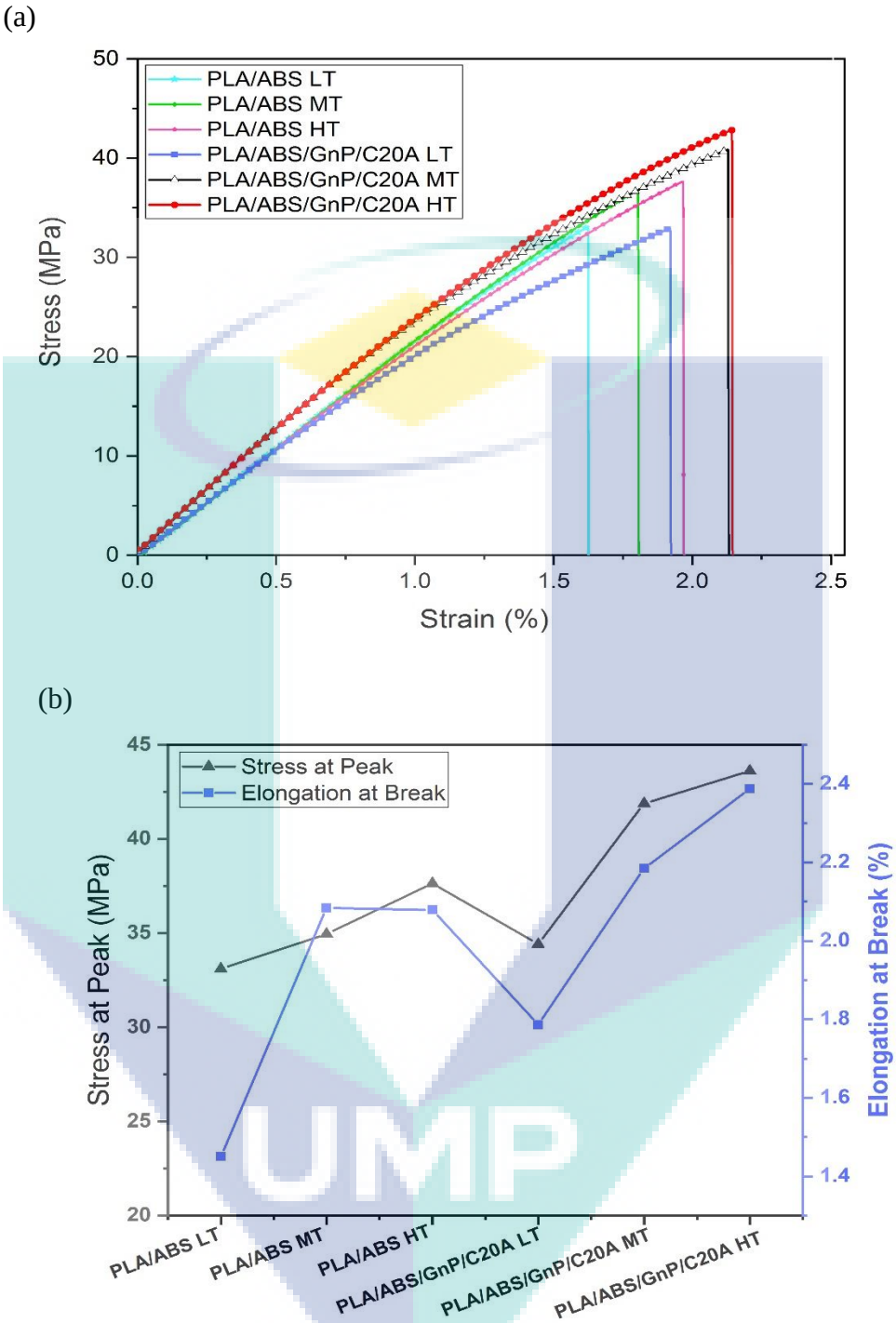

Figure 4.1 (a) Stress-strain curves of PLA/ABS and PLA/ABS/GnP/C20A across temperature profile and (b) Tensile strength and elongation at break curve as function of nanocomposites.

The same observation was illustrated in Figure 4.1 (b), where the elongation at break was enhanced with the addition of the fillers. There is elongation at break increment from 2.1% in both temperature profiles of PLA/ABS to 2.2% and 2.4% for PLA/ABS/GnP/C20A MT and PLA/ABS/GnP/C20A HT respectively. However, while prior researches like in Jollands and Gupta's (2010) and Gamez-Perez et. al. (2011) had found that nanoclay enhances the elongation at break attributed to the nanoparticles alignment, this increment was not as significant [60,61]. The reason may be attributed to the GnP brittle properties. The same

abnormal behaviour of PLA/ABS/GnP/C20A LT was also observed. Again, like in the tensile strength, the agglomeration of GnP is attributed to this behaviour.

On the other hand, the trend of Young's modulus as depicted in Figure 4.2 (c) shows an increment in value without the PLA/ABS/GnP/C20A abnormal behaviour. The Young's modulus increases both when the hybrid nanofiller was introduced and when the temperature profile increases. At MT and HT profile, the Young's Modulus increase by 23% and 18% respectively. Again, this finding is attributed to the dispersion of the GnP/C20A hybrid nanofiller in the PLA matrix. The higher aspect ratio and the large surface area of both the GnP and C20A results in this enhancement of Young's modulus.

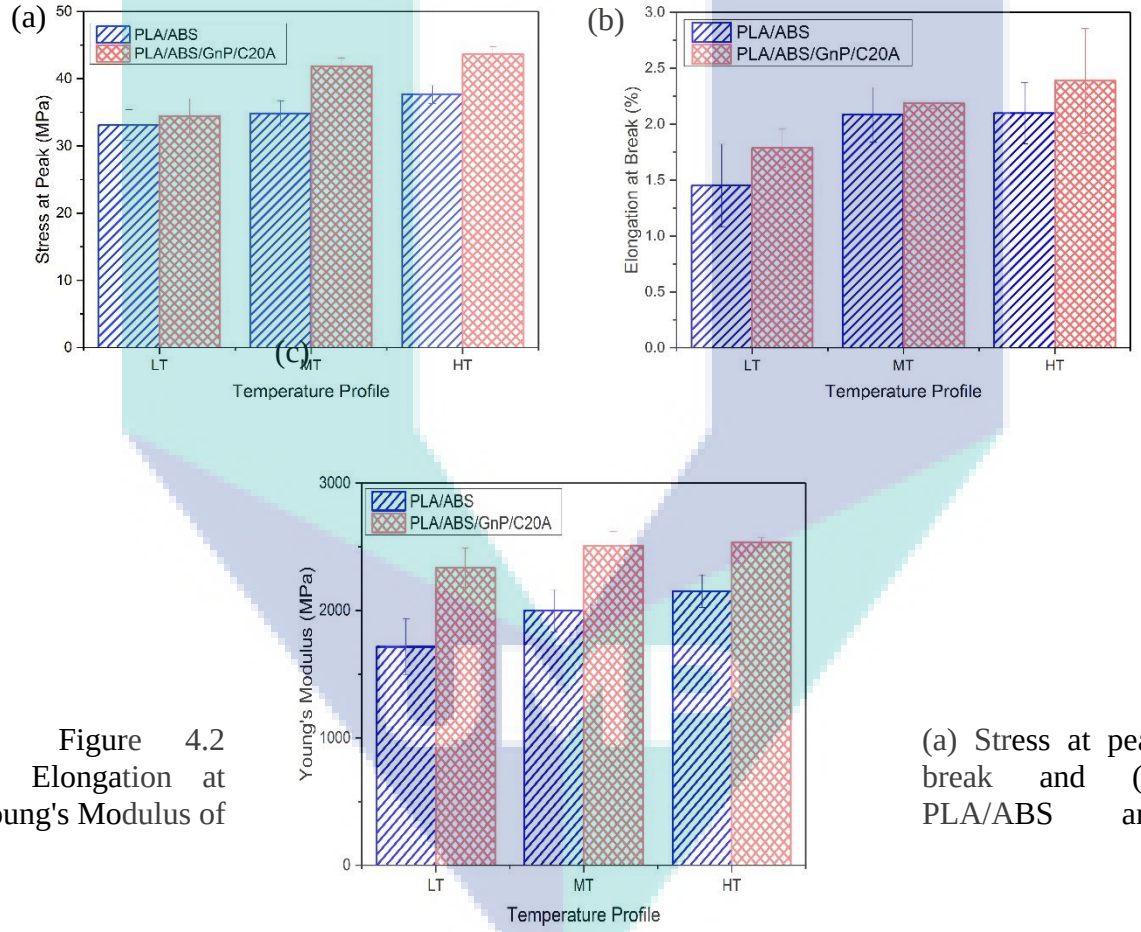

Figure 4.2 (a) Stress at peak (b) Elongation at break and (c) Young's Modulus of PLA/ABS and PLA/ABS/GnP/C20A nanocomposites as function of temperature profile.

The correlation of mechanical properties of stress at break, elongation at break and Young's modulus for PLA, ABS, PLA/ABS and PLA/ABS/GnP/MMT nanocomposites with different temperature condition are shown in Table 3. Note that there is no data for PLA/ABS at low temperature due to insufficient sample after few trials to get reliable data. From the previous studies, by the addition of the nanofillers in the polymer matrix will expect the increase of the mechanical properties of the nanocomposites. From this experiment, it was observed the significant change from PLA/ABS without nanofillers to with the nanofillers, as

shown in Figure 4.2. The stress at peak showed the highest value at low temperature that is 50.67 MPa compared to the other temperature condition. However, it was also noted that the value of stress at peak for medium and high temperature found to be the not much significant difference with the low temperature. Table 4.1 shows a value of the stress at peak for the nanocomposites.

The elongation at break for nanocomposites blends with different temperature condition is shown in Table 3. It is observed that the addition of nanofillers increased the elongation at break of 2.1%, 2.7%, 2.9% and 2.7% for unfilled, low, medium and high temperature with nanofillers loading, respectively as per shown in Figure 4.2 (a-c). It is also observed that for PLA/ABS/GnP/MMT nanocomposites, the medium temperature condition setting gave high elongation at break of 2.9% compared to the low and high temperature of 2.7%. Both stress at peak and elongation at break is also observed to have significant increase changes from PLA/ABS to PLA/ABS/GnP/MMT as shown in Figure 4.2 (a-b). While Figure 4.2 (c) showed Young's Modulus trend for all nanocomposites which observed to have an increasing trend from PLA/ABS to PLA/ABS/GnP/MMT. This is probably by adding the nanoclay and graphene into the polymer matrix, the brittleness characteristic of PLA which has very high modulus (3800MPa) has been improved. The incorporation of nanoclay also improves Young's modulus result of PLA/ABS/GnP compared to PLA/ABS which due to hydrogen bond in the functional group on the surface of nanoclay with carbonyl groups of the PLA and the dispersion of nanoclay in the polymer matrix.

Similar findings were reported by Cao et al. where they found that a small percentage of graphene contributed to the 26% increase in tensile strength and a 18% raise in Young's modulus [62].

Table 4.1. Mechanical properties of the PLA, ABS, PLA/ABS and PLA/ABS/GnP/C20A nanocomposites

Composition	**Young's Modulus [MPa]**	**Stress at Peak [MPa]**	**Elongation at Break [%]**
PLA/ABS LT	1715	32.9	1.5
PLA/ABS MT	1999	34.9	2.1
PLA/ABS HT	2152	37.6	2.1
PLA/ABS/GnP/C20A LT	2335	34.4	1.8
PLA/ABS/GnP/C20A MT	2506	41.9	2.2
PLA/ABS/GnP/C20A HT	2533	43.6	2.4

4.2 MMT/GNP dispersion and Morphology

It is known that reinforcing filler will increase tensile and modulus and heat deflection temperaures and it is governed by size and shape of the filler particles. Figures 3 to 5 depicted

the SEM micrograph obtained from the surface of the tensile test fractured site of the both PLA/ABS and PLA/ABS/GnP/C20A at all three temperature profiles. From the micrograph it can be seen that all the nanocomposites exhibit voids. The void formation indicates that the immiscibility and low interfacial adhesion of the polymer as commented by Boakaz et. al. [63].

From the micrograph, in PLA/ABS (Figure 4.3 a), only the void sizes in the LT profile (average of void of 1.451 µm) is obviously bigger in size and are much more uneven in comparison to the other temperature. This suggests that the fracture occurred at the interface between the 4 phases of the polymer (ABS consist of three polymers in blends). On the other hand, a more uniform dispersion of PLA was observed in the MT and HT profile of the PLA/ABS. In addition, the void size only varies slightly (average size of void of MT and HT are 0.533 µm and 0.726 µm respectively). These findings agree with the tensile results in which the difference was quite small but increases with the decrease in size of the void.

On the other hand, in the micrograph of the PLA/ABS/GnP/C20A (Figure 4.3 b), while the void sizes are similar (average size of void of LT, MT and HT are approximately 0.949 µm, 0.711 µm and 0.976 µm respectively) in all the temperature profiles, the dispersion of the GnP varies. The dispersion of graphene can be denoted by the graphitic layer structure seen in the micrograph (Gao et. al., 2017). The more the morphology is layered, the higher the extent of agglomeration of the GnP. The agglomeration of the GnP are clearly indicated in the LT profile by the highly layered and flaky surface seen in the micrograph. The agglomeration was quite severe explaining the dramatic decrease of the stress and the elongation at break when the fillers are introduced in the LT profile processing in comparison to the neat PLA/ABS nanocomposite. However, as the processing temperature was increased, the dispersion improved. This could be attributed to the high Van der Waal forces between the GnP sheets. Increasing the temperature increases the kinetic energy requires to break these forces and thus allows for better intercalation in the polymer matrices.

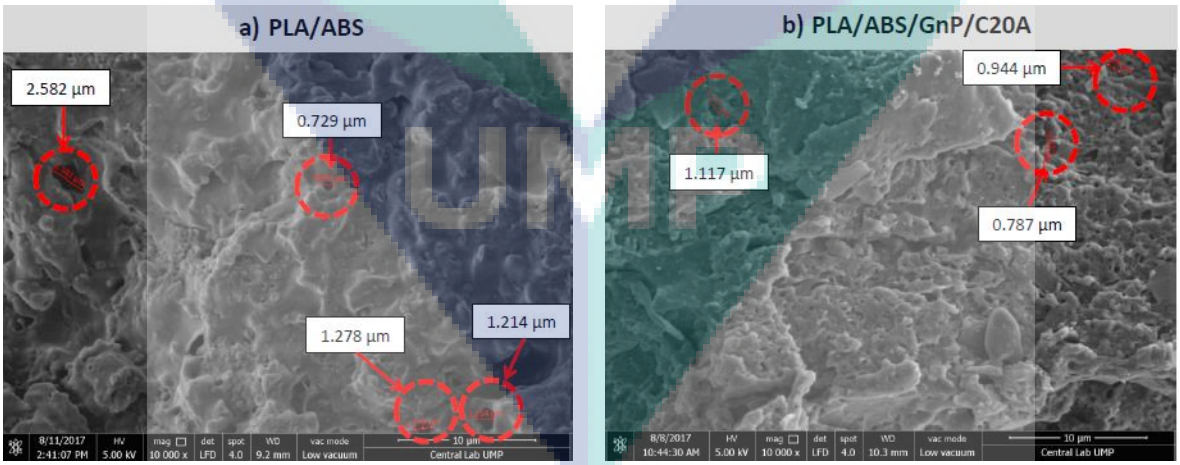

Figure 4.3 SEM micrograph taken from the surface of tensile fracture site at x10000 magnification for LT profile.

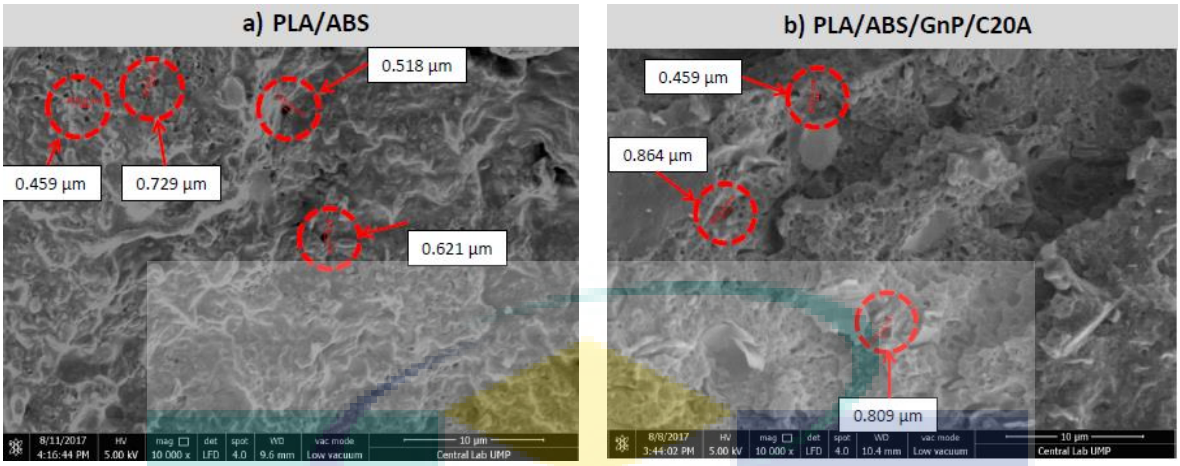

Figure 4.4 SEM micrograph taken from the surface of tensile fracture site at x10000 magnification for MT profile.

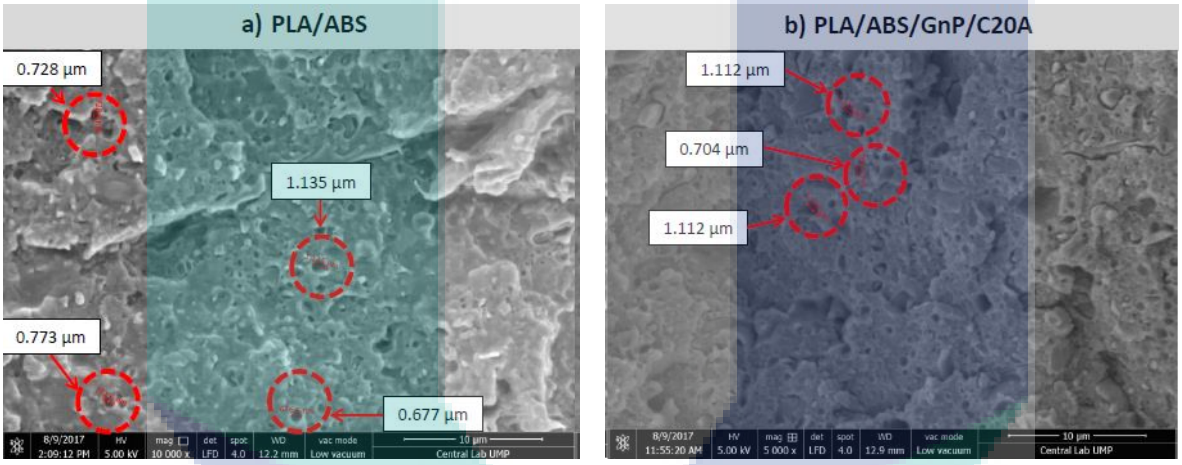

Figure 4.5 SEM micrograph taken from the surface of tensile fracture site at x10000 magnification for HT profile

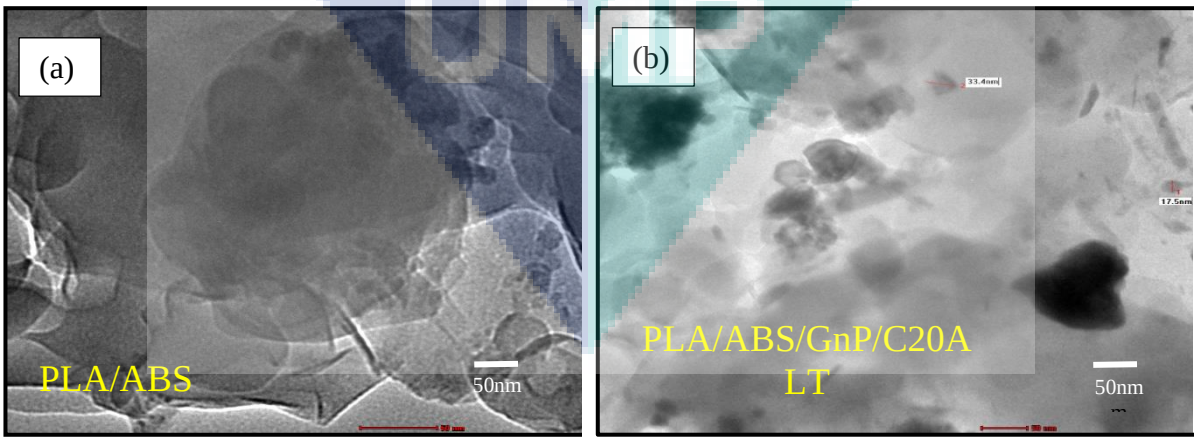

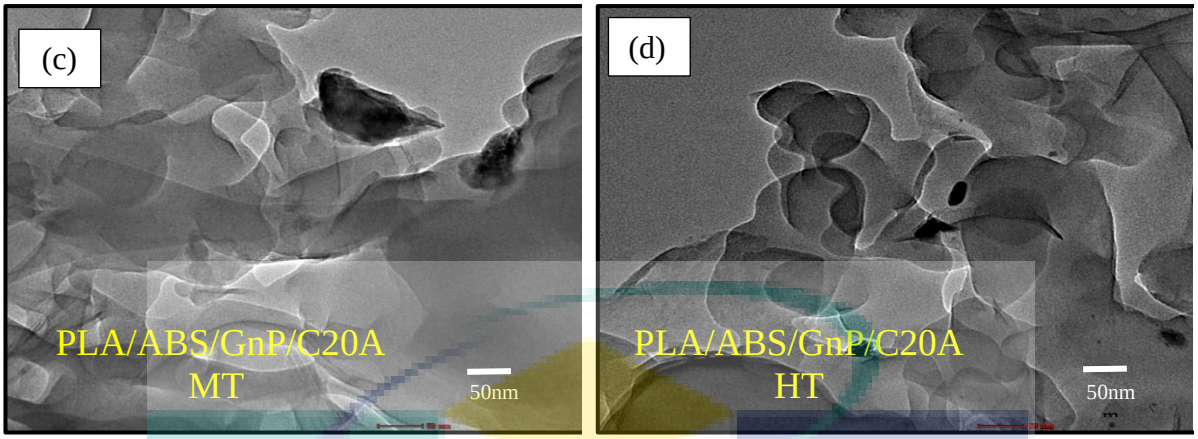

Figure 4.6 TEM images for (a) PLA/ABS/GnP/C20A LT profile (b) PLA/ABS MT profile (c) PLA/ABS/GnP/C20A MT profile and (d) PLA/ABS/GnP/C20A HT profile at 50 nm magnification

4.3 Fourier Transform Infrared (FTIR)

Fourier transform infrared spectra for PLA, ABS, PLA/ABS and PLA/ABS/GnP/C20A at LT/MT/HT temperature profiles are displayed in the Figure 4.7. The functional group interactions of the PLA with ABS, GnP and C20A through the shift of the absorption peak in specific regions was monitored. The characteristic peaks of PLA were at 1746, 2995, 2946 and 1080 cm^{-1} which are the frequency of C=O, -CH_3 asymmetric, -CH3 symmetric, and C-O functional groups respectively (Chieng et. al., 2014c). As for ABS, the characteristic frequency were at 2924 cm^{-1} for the asymmetric and symmetric CH2 stretch, 2237 cm^{-1} for C≡N stretch, as well as 966 cm^{-1} and 912 cm^{-1} for out-of-plane C-H stretch of butadiene [64].

Figures 4.7(a-d) depicted the FTIR spectrum of neat PLA, neat ABS, PLA/ABS LT and PLA/ABS/GnP/C20A LT. The nanocomposites exhibits the similar peaks that a nanocomposite of PLA and ABS should have without any other new peaks observed. This suggest that no chemical reaction occurs between any of the functional group which means the nanocomposites are purely of physical blends and thus are immiscible.

However, it was also noted from Figure 4.7 (c) and (d) that increasing the processing temperature profile increases the intensity of the peaks. According to the Beer-Lambert's Law [65], the intensity of the peak is related to either the concentration of the functional group or the thickness of the sample (thickness relates to the light path). Since the samples has similar thickness this could mean that the higher the processing temperature, the higher the concentration of the functional group in the sample. This could be due to the void formation that occurs during the sample moulding. On the other hand, the intensity difference when filler was introduced could be attributed to the filler agglomeration.

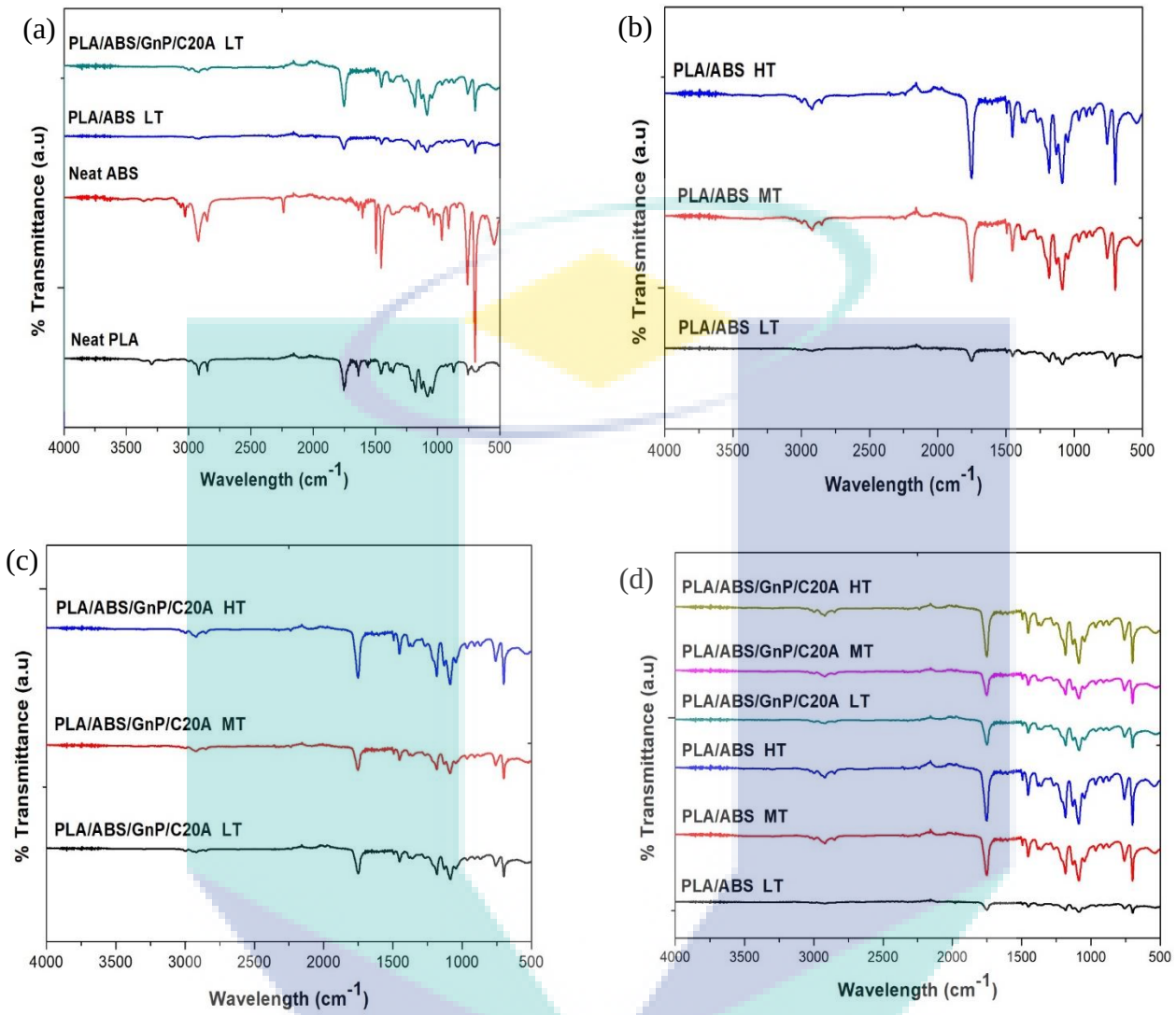

Figure 4.7 FTIR comparison (a) Neat PLA, Neat ABS, PLA/ABS at Low Temperature Profile and PLA/ABS/GnP/C20A at low Temperature Profile; (b) PLA/ABS across temperature profile; (c) PLA/ABS/GnP/C20A across temperature profile and (d) PLA/ABS and PLA/ABS/GnP/C20A across temperature profile

4.4 Thermal Analysis

Table 4.2 summarizes the thermal properties; the glass transitioning temperature, melting temperature and cold crystallization, of the neat PLA, neat ABS, PLA/ABS and PLA/ABS/GnP/C20A nanocomposites obtained from DSC. Note that T_{g1} was not available for most of the polymers since the peak, belonging to butadiene component in the ABS, was too close to the starting temperature. It was found that the nanocomposites possess multiple T_gs. This again indicates the immiscibility of the nanocomposite which is agreed by Fayt et. al. [66] who stated that immiscible polymer blends have multiple T_gs due to the phase separation of the polymers, resulting in low cohesive energy.

It was also noted that the melting temperature of the polymer blends are lower in comparison to the neat PLA and neat ABS. This could be due to drop in the degree of crystallinity as a result of the amorphous nature of ABS. The degree of crystallinity affects the melting point of polymer which agrees with findings by Wacharawichanant et. al. who found the melting point of PLA drops with addition of propylene-ethylene copolymer (PEC)[67]. He stated that this drop in melting point is due to the drop in the degree of crystallinity as result of the amorphous nature of PEC. However, this could not be concluded with the lack of crystallinity data.

In fact, if the blend components were immiscible, the Tg values of individual polymers would remain essentially unaffected. On the other hand, a completely miscible mixture would display a single Tg. It can, therefore, be concluded that the examined ABS/PC system shows a wide range of miscibility of its components, up to at least a concentration of ABS of 50%.

As shown in Table 4.2, the cold crystallization temperature of PLA/ABS blends at the medium temperature is about 95.0℃ and shift to around 92.5℃ after incorporation of the GnP. The combination effects of nucleation and diffusion-controlled growth processes resulted in the change of cold crystallization behavior in the PLA/ABS/GnP/MMT nanocomposites. Based on the study by Chieng et al., a slight change of PLA crystallinity after addition of GnP could not induce significant impact on the mechanical properties of the nanocomposites (30).On the other hand, the homogeneous dispersion of GnP in the polymer matrix and strong interactions between both components can influence the significant changes of the strength and modulus of PLA/ABS nanocomposites.

Organoclay addition of 2 phr to ABS does not have any obvious effect on the T_g of SAN phase, whereas a decrease was recorded in the case of all the examined ABS/PC blends. Tiwari and Natarajan [68] observed that Tg of ABS hybrids remain unaffected by the incorporation of unmodified or organically modified montmorillonite (Cloisite 6A, 10A, 20A, and 25A) or laponite at 4% loading, independently on the particle and platelet size. On the other hand, Yeh et al. [69] found that the incorporation of organoclay results in an increase of T_g with respect to that of neat ABS and interpreted this effect by the confinement of intercalated polymer chains within the organoclay galleries, which prevents the segmental motions of polymer chains [69].

Table 4.2 DSC data on the neat PLA, neat ABS, PLA/ABS and PLA/ABS/GnP/C20A nanocomposites

Composition	**T_{g1}, T_{g2}, T_{g3} [°C]**	**T_c [°C]**	**T_m [°C]**

PLA	60	-	170.2
ABS	-90.3,67.5,140	-	169.3
PLA/ABS LT	- , 62.5,150.0	92.5	166.0
PLA/ABS MT	- , 62.5, 150.0	95.0	165.8
PLA/ABS HT	- , 60.0, 150.0	90.0	165.1
PLA/ABS/GnP/C20A LT	- , 62.5, 150.0	95.0	166.1
PLA/ABS/GnP/C20A MT	- , 60.0,150.0	92.5	165.7
PLA/ABS/GnP/C20A HT	- , 62.5, 150.0	92.5	165.9

Table 4.3 TGA data on the neat PLA, neat ABS, PLA/ABS and PLA/ABS/GnP/C20A nanocomposites

Composition	**Onset Temperature (°C)**	**Peak Temperature (°C)**	**End Temperature (°C)**
PLA	330.5	352.9	368.6
ABS	388.5	410.6	464.3
PLA/ABS LT	317.0, 379.6	334.8, 400.7	476.5
PLA/ABS MT	316.5, 376.7	333.3, 400.3	491.5
PLA/ABS HT	315.4, 377.2	333.2, 402.6	486.6
PLA/ABS/GnP/C20A LT	334.3, 387.2	350.6, 404.9	483.9
PLA/ABS/GnP/C20A MT	336.0, 390.0	351.6, 404.8	482.6
PLA/ABS/GnP/C20A HT	337.9, 389.5	352.4, 407.4	482.5

The degradation behaviour of PLA, ABS, PLA/ABS and PLA/ABS/GnP/C20A nanocomposites are given in the Figure 4.8 and Table 4.3. The onset temperature is represented by the start of weight loss while the end temperature is the temperature at the end of degradation. Since this is a blend of two polymers, the polymer blends results having two degradation onset temperature and peak temperature. However, since the onset of the ABS occurs before PLA fully degraded, the end temperature recorded are for full degradation of the polymer blends. In general, it was found that the degradation temperature of both PLA and ABS decreases when the polymer is blended which is expected of a polymer blend. There are no significant findings observed when comparing the temperature profile of the polymers. However, the addition of the fillers increases the thermal stability of the PLA/ABS nanocomposites as depicted by the increase in onset temperature and the peak temperature. This could be due to the nanoparticles reinforcement of the nanofillers which both possessing higher decomposition temperature. This finding is in agreement with studies by Fukushima et.

al. when they prepared PLA based nanocomposites by using two different nanofillers: expanded graphite and organically modified montmorillonite. There are also no significant findings observed on the end temperature of the polymers as all the nanocomposites shows similar or small difference in end temperature.

It can be seen that the decomposition of PLA started at 330.5℃ and completed at 368.6℃ while PLA/ABS blends at medium temperature condition started to decompose at 316.5℃ and 376.7 ℃ and completed at 476.5℃ and PLA/ABS/GnP/MMT blends at medium temperature started to decompose at 325.7℃ and 390.2℃ and completed at 487.3℃ and 499.8℃. From the result, the onset of degradation of PLA/ABS and PLA/ABS/GnP/MMT started slower than PLA. Thermograms of PLA/ABS/GnP/MMT shows high thermal stability than PLA/ABS blends. This is probably due to dispersion state of MMT layers in the polymer matrix. The graphene improved the thermal stability of PLA/ABS matrix due to the intrinsic characteristic of the graphene leads to great enhancement of the thermal stability of the polymer matrix. Graphene sheets take a role of thermal barriers and improve the thermal stability of polymer matrix [71,72]. With the incorporation of GnP into polymer matrix will enhance the overall material's thermal stability. The layer structure gives a greater barrier effect to inhibit the evaporation of the volatile degradation products generated in thermal decomposition of the nanocomposite [70]. The phenomena was responsible to contribute to the enhancement of thermal stability for PLA/ABS/GnP/MMT [73]. It is worth noting that the compatibilizing action of C20A contributed to the decrease in the interfacial tension and hence leads to a remarkable in mechanical and thermal properties of the PLA/ABS/GnP/C20A nanocomposites.

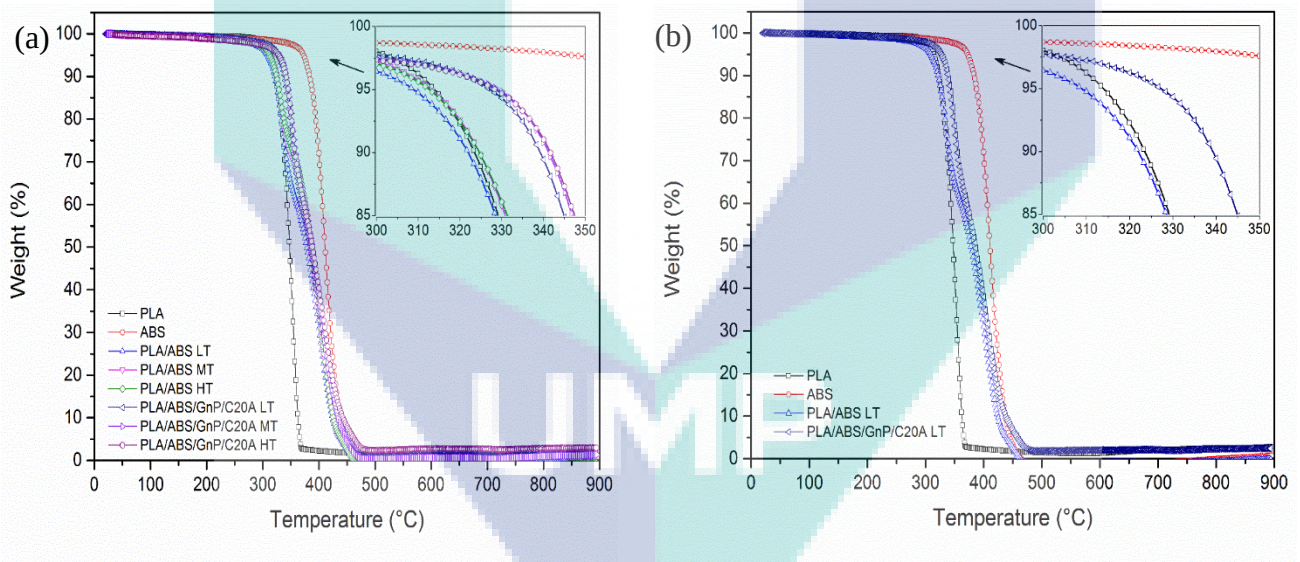

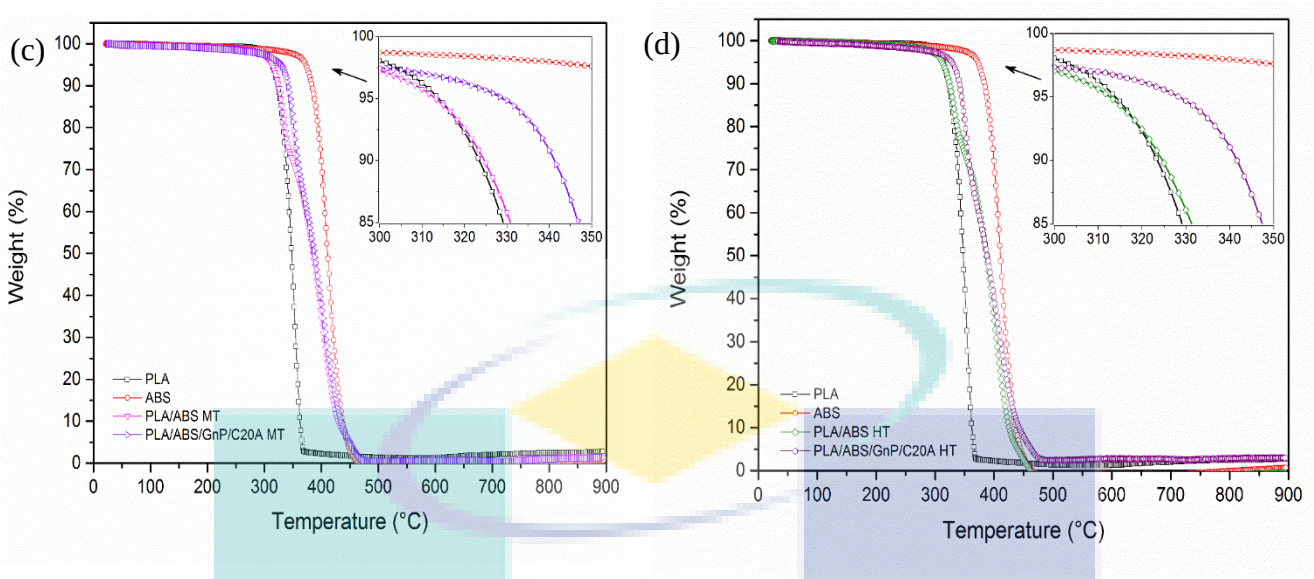

Figure 4.8. TGA curves on (a) neat PLA, neat ABS, PLA/ABS and PLA/ABS/GnP/C20A nanocomposite; (b) LT profile; (c) MT profile and (d) HT profile

4.5. Conclusion

The PLA/ABS/GnP/C20A nanocomposites had been successfully prepared and the effect of processing temperature profile on the mechanical, morphological and thermal properties of PLA/ABS and PLA/ABS/GnP/C20A nanocomposites were investigated. The studies also found that increasing the temperature profile enhances the mechanical properties in PLA/ABS/GnP/C20A while no significant findings were observed in PLA/ABS. Tensile strength was observed to increase by 20% and 16% in MT and HT profile respectively while the young modulus was increase by 23% and 18% in MT and HT profile respectively. The enhancement of the properties was contributed to the dispersion of the filler. Increasing temperature results in better dispersion of the fillers as can be seen from the morphological characterisation by SEM and TEM. However, while the elongation at break also increases with increasing temperature, the enhancement was insignificant maybe due to the brittle nature of graphene. However, from the FTIR result exhibits not many significant changes and no chemical reaction happens in any functional group and DSC analysis also exhibits not many significant changes via different temperature condition.

On the other hand, in terms of thermal analysis, there is no significant finding was observed on the effect of the temperature profile although it was noted that the melting point was slightly increased when fillers was introduced. The same occurs in the thermal stability, in which the incorporation of filler increases the thermal stability of the nanocomposites but no significant observation made across temperature profile.

REFERENCES

[1] Nofar, M., Sacligil, D., Carreau, P. J., Kamal, M. R. and Heuzey, M.-C., \Poly(lactic acid) Blends: Processing, Properties and Appli cations", Int. J. Biol. Macromol., 125, 307–360 (2019), PMid:30528997; DOI:10.1016/j.ijbiomac.2018.12.002

[2] Bijarimi, M., Ahmad, S. and Alam, A. K. M. M., \Toughening Effect of Liquid Natural Rubber on the Morphology and Thermo-Mechanical Properties of the Poly(lactic acid) Ternary Blend", Polymer Bull., 74, 3301 –3317 (2017), DOI:10.1007/s00289-016-1889-7

[3] Bitinis, N., Verdejo, R., Maya, E. M., Espuche, E., Cassagnau, P. and Lopez-Manchado, M. A., \Physicochemical Properties of Organoclay Filled Polylactic Acid/Natural Rubber Blend Bionanocomposites", Compos. Sci. Technol., 72, 305–313 (2012), DOI:10.1016/j.compscitech.2011.11.018

[4] Pluta, M., Paul, M. A., Alexandre, M. and Dubois, P., \Plasticized Polylactide/Clay Nanocomposites. I. The Role of Filler Content and its Surface Organo-Modification on the Physico-Chemical Properties", J. Polym. Sci., Part B: Polym. Phys., 44, 299–311 (2006), DOI:10.1002/polb.20694

[5] Vadori, R., Misra, M. and Mohanty, A. K., \Sustainable Biobased Blends from the Reactive Extrusion of Polylactide and Acrylonitrile Butadiene Styrene", J. Appl. Polym. Sci., 133, (2016), DOI:10.1002/app.43771

[6] Vadori, R., Misra, M. and Mohanty, A. K., \Statistical Optimization of Compatibilized Blends of Poly(lactic acid) and Acrylonitrile Butadiene Styrene", J. Appl. Polym. Sci., 134, (2017), DOI:10.1002/app.44516

[7] Li, Y., Shimizu, H., \Improvement in Toughness of Poly(L-lactide) (PLLA) through Reactive Blending with Acrylonitrile–Butadiene– Styrene Copolymer (ABS): Morphology and Properties", Eur. Polym. J., 45, 738–746 (2009), DOI:10.1016/j.eurpolymj.2008.12.010

[8] Choe, I.-J., Lee, J. H., Yu, J. H. and Yoon, J.-S., \Mechanical Properties of Acrylonitrile–Butadiene–Styrene Copolymer/Poly(L-lactic acid) Blends and their Composites", J. Appl. Polym. Sci., 131, (2014), DOI:10.1002/app.40329

[9] Dong, W., He, M., Wang, H., Ren, F., Zhang, J., Zhao, X. and Li, Y., \PLLA/ABS Blends Compatibilized by Reactive Comb Polymers: Double Tg Depression and Significantly Improved Toughness", ACS Sustainable Chem. Eng., 3, 2542 –2550 (2015), DOI:10.1021/acssuschemeng.5b00740

[10] Wu, N., Zhang, H., \Toughening of Poly(L-lactide) Modified by a Small Amount of Acrylonitrile–Butadiene–Styrene Core-Shell Copolymer", J. Appl. Polym. Sci., 132, (2015), DOI:10.1002/app.42554

[11] Alexandre, M., Dubois, P., \Polymer-Layered Silicate Nanocomposites: Preparation, Properties and Uses of a New Class of Materials", Mater. Sci. Eng., R, 28, 1–63 (2000), DOI:10.1016/S0927-796X(00)00012-7

[12] Arroyo, O. H., Huneault, M. A., Favis, B. D. and Bureau, M. N., \Processing and Properties of PLA/Thermoplastic Starch/Montmorillonite Nanocomposites", Polym. Compos., 31, 114–127 (2010), DOI:10.1002/pc.20774

[13] Bijarimi, M., Amirul, M., Norazmi, M., Ramli, A., Desa, M. S. Z., Desa, M. A. and Abu Samah, M. A., \Preparation and Characterization of Poly(lactic acid) (PLA)/Polyamide 6 (PA6)/Graphene Nanoplatelet (GNP) Blends Bio-Based Nanocomposites", Mater. Res. Express, 6, (2019), DOI:10.1088/2053-1591/ab05a3

[14] Coiai, S., Cicogna, F., De Santi, A., Pérez Amaro, L., Spiniello, R., Signori, F., Fiori, S., Oberhauser, W. and Passaglia, E., \MMT and LDH Organo-Modification with Surfactants Tailored for PLA Nanocomposites", eXPRESS Polym. Lett., 11, 163 –175 (2017), DOI:10.3144/expresspolymlett.2017.18

[15] Gonçalves, C., Pinto, A., Machado, A. V., Moreira, J., Gonçalves, I. C. and Magalhães, F., \Biocompatible Reinforcement of Poly(lactic acid) with Graphene Nanoplatelets", Polym. Compos., (2016), DOI:10.1002/pc.24050

[16] Jalalvandi, E., Majid, R., Ghanbari, T. and Ilbeygi, H., \Effects of Montmorillonite (MMT) on Morphological, Tensile, Physical Barrier Properties and Biodegradability of Polylactic Acid/Starch/ MMT Nanocomposites", J. Thermoplast. Compos. Mater., 28, 496–509 (2015), DOI:10.1177/0892705713486129

[17] Keramati, M., Ghasemi, I., Karrabi, M., Azizi, H. and Sabzi, M., \Incorporation of Surface Modified Graphene Nanoplatelets for Development of Shape Memory PLA Nanocomposite", Fibers Polym., 17, 1062–1068 (2016), DOI:10.1007/s12221-016-6329-7

[18] Li, S., Li, Z., Burnett, T. L., Slater, T. J. A., Hashimoto, T. and Young, R. J., \Nanocomposites of Graphene Nanoplatelets in Natural Rubber: Microstructure and Mechanisms of Reinforcement", J. Mater. Sci., 52, 9558 –9572 (2017), DOI:10.1007/s10853-017-1144-0

[19] Manafi, P., Ghasemi, I., Karrabi, M., Azizi, H. and Ehsaninamin, P., \Effect of Graphene Nanoplatelets on Crystallization Kinetics of Poly(lactic acid)", Soft Mater., 12, 433–444 (2014), DOI:10.1080/1539445X.2014.959598

[20] Pinto, A. M., Gonçalves, C., Gonçalves, I. C. and Magalhães, F. D., \Effect of Biodegradation on Thermo-Mechanical Properties and Biocompatibility of Poly(lactic acid)/Graphene Nanoplatelets Composites", Eur. Polym. J., 85, 431–444 (2016), DOI:10.1016/j.eurpolymj.2016.10.046

[21] Sabzi, M., Jiang, L. and Nikfarjam, N., \Graphene Nanoplatelets as Rheology Modifiers for Polylactic Acid: Graphene Aspect-RatioDependent Nonlinear Rheological Behavior", Ind. Eng. Chem. Res., 54, 8175–8182 (2015), DOI:10.1021/acs.iecr.5b01863

[22] Scaffaro, R., Botta, L., Maio, A. and Gallo, G., \PLA Graphene Nanoplatelets Nanocomposites: Physical Properties and Release Kinetics of an Antimicrobial Agent", Composites Part B, 109, 138–146 (2017), DOI:10.1016/j.compositesb.2016.10.058

[23] Sharma, N., Alam, S. N., Ray, B. C., Yadav, S. and Biswas, K., \SilicaGraphene Nanoplatelets and Silica-MWCNT Composites: Microstructure and Mechanical Properties", Diamond Relat. Mater., 87, 186–201 (2018), DOI:10.1016/j.diamond.2018.06.009

[24] Young, R. J., Liu, M., Kinloch, I. A., Li, S., Zhao, X., Vallés, C. and Papageorgiou, D. G., \The Mechanics of Reinforcement of Polymers by Graphene Nanoplatelets", Compos. Sci. Technol., (2018), DOI:10.1016/j.compscitech.2017.11.007

[25] Fu, Y., Liu, L., Zhang, J. and Hiscox, W. C., \Functionalized Graphenes with Polymer Toughener as Novel Interface Modifier for Property-Tailored Polylactic Acid/Graphene Nanocomposites", Polymer, 55, 6381 –6389 (2014), DOI:10.1016/j.polymer.2014.10.014

[26] Bouakaz, B. S., Pillin, I., Habi, A. and Grohens, Y., \Synergy between Fillers in Organomontmorillonite/Graphene–PLA Nanocomposites", Appl. Clay Sci., 116 – 117, 69 –77 (2015), DOI:10.1016/j.clay.2015.08.017

[27] Nuona, A., Li, X., Zhu, X., Xiao, Y., & Che, J. (2014). Starch/Polylactide Sustainable Composites: Interface Tailoring with Graphene Oxide. *Composites: Part A, 69 (2015), 247–254.* http://dx.doi.org/10.1016/j.compositesa.2014.11.025

[28] Hamad, K., Kasseem, M., Yang, H. W., Deri, F., & Ko, Y. G. (2014). Properties and Medical Applications of Polylactic Acid: A Review. *eXPRESS Polymer Letters Vol 9, No 5 (2015), 435-455.* doi:10.3144/expresspolymlett.2015.42

[29] Garlotta, D. (2002). A Literature review of Poly(Lactic Acid). *Journal of Polymers and the Environment, Vol. 9, No 2 (2002).* doi:1566-2543/01/0400-0063/0

[30] Sun, S., Zhang, M., Zhang, H., & Zhang, X. (2011). Polylactide Toughening with Epoxy-functionalized Grafted Acrylonitrile-butadiene-styrene Particles. *Journal of Applied Polymers Science 122, 2992-2999.* doi:10.1002/app.34111

[31] Bhattacharya, M. (2016). Polymer Nanocomposites – A Comparison between Carbon Nanotubes, Graphene and Clay as nanofillers. *Materials 2016, 9, 262.* doi:10.3390/ma9040262

[32] Kuilla, T., Bhadra, S., Yao, D., Kim, N. H., Bose, S., & Lee, J. H. (2010). Recent Advances in Graphene Based Polymer Composites. Progress in Polymer Science, 35 (2010), 1350–1375. doi:10.1016/j.progpolymsci.2010.07.005

[33] Norazlina, H. & Kamal, Y. (2014). Graphene Modifications in Polylactic Acid Nanocomposites: A Review. *Polym. Bull. (2015) 72:931–961*. doi: 10.1007/s00289-015-1308-5

[34] Singh, K., Ohlan, A., & Dawan, S.K. (2012). Polymer-Graphene Nanocomposites: Preparation, Characterization, Properties, and Applications. *Nanocomposites - New Trends and Developments,37-71*. http://dx.doi.org/10.5772/50408

[35] Conroy, J., Verma, N. K., Smith, R. J., Rezvani, E., Duesberg, G. S., Coleman, J. N., & Volkov, Y. (2014). Biocompatibility of Pristine Graphene Monolayers, Nanosheets and Thin Films. https://arxiv.org/pdf/1406.2497

[36] Marquis, D. M., Guillaume, E., & Chivas-Joly, C. (2011). Propertiesof Nanofillers in Polymer, Nanocomposites and Polymers with Analytical Methods. Dr. John Cuppoletti (Ed.), ISBN: 978-953-307-352-1, InTech. http://www.intechopen.com/books/nanocomposites-and-polymers-with -analytical-methods/properties-of-nanofillers-in-polymer.

[37] Tan, B., & Thomas, N. L. (2016). A Review of the Water Barrier Properties of Polymer/Clay and Polymer/Graphene Nanocomposites. *Journal of Membrane Science 514 (2016), 595–612.* http://dx.doi.org/10.1016/j.memsci.2016.05.026

[38] Okamoto, M. (2016). Recent Advancess in Polymer/LayeredSilicate Nanocomposites: An Overview from Science to Technology. *Materials Science and Technology 22 (2006), 756-779.* http://dx.doi.org/10.1179/174328406X101319

[39] Sinha, S. R., & Okamoto, M. (2003). Polymer/Layered Silicate Nanocomposites: A Review from Preparation to Processing. *Progress in Polymer Science 28 (2003), 1539-1641.* https://doi.org/10.1016/j.progpolymsci.2003.08.002

[40] Kamal, Y. (2009). Subsurface and Bulk Mechanical Properties of Polyurethane Nanocomposite Films. *Loughborough University Institutional Repository*. https://dspace.lboro.ac.uk/2134/6313

[41] Bhattacharya, M. (2016). Polymer Nanocomposites – A Comparison between Carbon Nanotubes, Graphene and Clay as nanofillers. *Materials 2016, 9, 262.* doi:10.3390/ma9040262

[42] Krishnamoorti, R.K., & Manias, E. (1999). Polymer-Silicate Nanocomposites: Model Systems for Confined Polymers and Polymer Brushes. *Advanced in Polymer Science 138 (1999), 107-147.* doi:10.1007/3-540-69711-X_3

[43] Roy, S., Srivastaval, S. K., Pionteck, J., & Mittal, V. (2013). Montmorillonite–Multiwalled Carbon Nanotube Nanoarchitecture Reinforced Thermoplastic Polyurethane. *Polymer Composites 37 (6),1775–1785.* doi:10.1002/pc.23350

[44] Fukushima, K., Murariu, M., Camino, G., & Dubois, P. (2010). Effect of Expanded Graphite/Layered-Silicate Clay on Thermal, Mechanical and Fire Retardant Properties of Poly(Lactic Acid). *Polymer Degradation and Stability 95 (6), 1063-1076.* https://doi.org/10.1016/j.polymdegradstab.2010.02.029

[45] Iman, M & Maji, T. K. (2010) Effect of Crosslinker and Nanoclay on Jute Fabric Reinforced Soy Flour Green Composite. *Applied Polymer Science 127 (5), 3987–3996.* doi:10.1002/app.37713

[46] Liu, R., Cao, J., Peng, Y., & Chen, Y. (2014). Physical, Mechanical, and Thermal Properties of Micronized Organo-Montmorillonite Suspension Modified Wood Flour/Poly(Lactic Acid) Composites. *Polymer Composites 36 (4), 731–738.* doi:10.1002/pc.22992

[47] Najafi, N., Heuzey, M. C., & Carreau, P. J. (2012). Polylactide (PLA)-clay Nanocomposites Prepared by Melt Compounding in the Presence of a Chain Extender. *Composites Science and Technology 72 (2012), 608–615.* doi:10.1016/j.compscitech.2012.01.005

[48] Das, T. K., & Prusty, S. (2016). Graphene-Based Polymer Composites and Their Applications. *Polymer-Plastics Technology and Engineering, 52:4, 319-331.* doi:10.1080/03602559.2012.751410

[49] Pavlidou, S., & Papaspyrides, C. D. (2008). A Review on Polymer-Layered Silicate Nanocomposites. *Progress in Polymer Science 33 (2008), 1119-1198.* doi:10.1016/j.progpolymsci.2008.07.008

[50] Gamez-Perez, J., Nascimento, L., Bou, J. J., Franco-Urquiza, E., Santana, O. O., Carrasco, F., & Maspoch, M. Ll. (2010). Influence of Crystallinity on the Fracture Toughness of Poly(Lactic Acid)/Montmorillonite Nanocomposites Prepared by Twin-Screw Extrusion. *Journal of Applied Polymer Science 120, 896-905.* doi:10.1002/app.33191

[51] Wang, B., Wan, T., & Zeng, W. (2012). Rheological and Thermal Properties of Polylactide/Organic Montmorillonite Nanocomposites. *Journal of Applied Polymer Science 125 (2), E364-E371.* doi:10.1002/app.36770

[52] Paul, A., Delcourt, C., Alexandre, M., Degée, P., Monteverde, F., & Dubois, P. (2005). Polylactide/Montmorillonite Nanocomposites: Study of the Hydrolytic Degradation. *Polymer Degradation and Stability 87 (2005), 535-542.* https://doi.org/10.1016/j.polymdegradstab.2004.10.011

[53] Cao, Y., Feng, J., & Wu, P. (2010). Preparation of Organically Dispersible Graphene Nanosheet Powders through a Lyophilization Method and Their Poly(Lactic Acid) Composites. *Carbon 48 (2010) 3834 – 3839.* doi:10.1016/j.carbon.2010.06.048

[54] Pinto, M., Cabral., J., Tanaka, D. A. P., Mendes, A. M., Magalhaes, F. D. (2012). Effect Of Incorporation of Graphene Oxide and Graphene Nanoplatelets on Mechanical and Gas Permeability Properties of Poly(Lactic Acid) Films. *Polymer International 62 (1), 33–40.* doi:10.1002/pi.4290

[55] Bouakaz, B. S., Pillin, I., Habi, A., and Grohens, Y. (2015). Synergy between Fillers in Montmorillonite/graphene-PLA Nanocomposites. *Applied Clay Science, 116-117 (2015), 69-77.* doi:10.1016/j.clay.2015.08.017

[56] Kim, I. H., & Jeong, Y. G. (2010). Polylactide/Exfoliated Graphite Nanocomposites with Enhanced Thermal Stability, Mechanical Modulus, and Electrical Conductivity. *Journal of Polymer Science Part B Polymer Physics 48, 850–858.* doi:10.1002/polb.21956

[57] Mat Desa, M. S. Z., Hassan, A., Arsad, A., & Mohammad, N. N. B. (2014). Mechanical Properties of Poly(lactic) acid/ multiwalled Carbon Nanotubes

Nanocomposites. *Materials Research Innovations, 18 (2014).* doi:10.1179/1432891714Z.000000000924

[58] Fukushima K, Murariu M, Camino G, Dubois P. Effect of expanded graphite/layered-silicate clay on thermal, mechanical and fire retardant properties of poly(lactic acid). Polymer Degradation and Stability. 2010;95(6):1063-76.

[59] Bouakaz BS, Pillin I, Habi A, Grohens Y. Synergy between fillers in organomontmorillonite/graphene–PLA nanocomposites. Applied Clay Science. 2015;116-117:69-77.

[60] Gamez-Perez J, Nascimento L, Bou JJ, Franco-Urquiza E, Santana OO, Carrasco F, et al. Influence of crystallinity on the fracture toughness of poly(lactic acid)/montmorillonite nanocomposites prepared by twin-screw extrusion. Journal of Applied Polymer Science. 2011;120(2):896-905.

[61] Jollands M, Gupta RK. Effect of mixing conditions on mechanical properties of polylactide/montmorillonite clay nanocomposites. Journal of Applied Polymer Science. 2010;118(3):1489-93.

[62] Cao Y, Feng J, Wu P. Preparation of organically dispersible graphene nanosheet powders through a lyophilization method and their poly(lactic acid) composites. Carbon. 2010;48(13):3834-9.

[63] Bouakaz BS, Habi A, Grohens Y, Pillin I. Organomontmorillonite/graphene-PLA/PCL nanofilled blends: New strategy to enhance the functional properties of PLA/PCL blend. Applied Clay Science. 2017;139:81-91.

[64] Ma H, Wang J, Fang Z. Cross-linking of a novel reactive polymeric intumescent flame retardant to ABS copolymer and its flame retardancy properties. Polymer Degradation and Stability. 2012;97(9):1596-605.

[65] Swinehart DF. The Beer-Lambert Law. Journal of Chemical Education. 1962;39(7):333.

[66] Fayt R, Hadjiandreou P, Teyssie P. Molecular design of multicomponent polymer systems. VII. Emulsifying effect of poly(ethylene–b–styrene) copolymer in high-density polyethylene/polystyrene blends. Journal of Polymer Science: Polymer Chemistry Edition. 1985;23(2):337-42.

[67] Wacharawichanant S, Ounyai C, Rassamee P, editors. Effects of organoclay to miscibility, mechanical and thermal properties of poly(lactic acid) and propylene-ethylene copolymer blends. IOP Conference Series: Materials Science and Engineering; 2017.

[68] Tiwari, R. R., Natarajan, U., \Effect of Organic Modifiers and Silicate Type on Filler Dispersion, Thermal, and Mechanical Properties of ABS-Clay Nanocomposites", J. Appl. Polym. Sci., 110, 2374 – 2383 (2008), DOI:10.1002/app.28699

[69] Yeh, J. M., Chen, C. L., Huang, C. C., Chang, F. C., Chen, S. C., Su, P. L., Kuo, C. C., Hsu, J. T., Chen, B. and Yu, Y. H., \Effect of Organoclay on the Thermal Stability, Mechanical Strength, and Surface Wettability of Injection-Molded ABS-Clay Nanocomposite Materials Prepared by Melt Intercalation", J. Appl. Polym. Sci., 99, 1576–1582 (2006), DOI:10.1002/app.22329

[70] Chieng B, Ibrahim N, Yunus W, Hussein M, Then Y, Loo Y. Effects of Graphene Nanoplatelets and Reduced Graphene Oxide on Poly(lactic acid) and Plasticized Poly(lactic acid): A Comparative Study. Polymers. 2014;6(8):2232.

[71] Chieng BW, Ibrahim NA, Wan Yunus WMZ, Hussein MZ. Effects of graphene nanopletelets on poly(lactic acid)/poly(ethylene glycol) polymer nanocomposites. Advanced Materials Research2014. p. 136-9.

[72] Chieng BW, Ibrahim NA, Wan Yunus WMZ, Hussein MZ, Silverajah VSG. Graphene nanoplatelets as novel reinforcement filler in poly(lactic acid)/epoxidized palm oil green nanocomposites: Mechanical Properties. International Journal of Molecular Sciences. 2012;13(9):10920-34.

[73] Jiajie L, Yi H, Long Z, Yan W, Yanfeng M, Tianyin G, et al. Molecular-Level Dispersion of Graphene into Poly(vinyl alcohol) and Effective Reinforcement of their Nanocomposites. Advanced Functional Materials. 2009;19(14):2297-302.